Modeling the Sulfate Aerosol Evolution after Recent Moderate Volcanic Activity, 2008-2012

Christina Brodowsky[1], Timofei Sukhodolov[2], Aryeh Feinberg[1], Michael Höpfner[3], Thomas Peter[4], Andrea Stenke[5], and Eugene Rozanov[6]

[1]Swiss Federal Institute of Technology in Zurich
[2]PMOD/WRC
[3]Karlsruhe Institute of Technology
[4]Swiss Federal Institute of Technology (ETH)
[5]Institute for Atmospheric and Climate Research
[6]Physikalisch-Meteorologisches Observatorium Davos and World Radiation Center

November 24, 2022

Abstract

Volcanic activity is a main natural climate forcing and an accurate representation of volcanic aerosols in global climate models is essential. This is, however, a complex task involving many uncertainties related to the magnitude and vertical distribution of volcanic emissions as well as in observations used for model evaluation. We analyse the performance of the aerosol-chemistry-climate model SOCOL-AERv2 for three medium-sized volcanic eruptions. We investigate the impact of differences in the volcanic plume height and SO2 content on the stratospheric aerosol burden. The influence of internal model variability and dynamics are addressed through an ensemble of free-running and nudged simulations at different vertical resolutions. Comparing the modeled evolution of the stratospheric aerosol loading to satellite measurements reveals a good performance of SOCOL-AERv2. However, the large spread in emission estimates leads to differences in the simulated aerosol burdens resulting from uncertainties in total emitted sulfur and the vertical distribution of injections. The tropopause height varies among the free-running simulations, affecting model results. Conclusive model validation is complicated by uncertainties in observations. In nudged mode, changes in convection and tropospheric clouds affect SO2 oxidation paths and cross-tropopause transport, leading to increased burdens. This effect can be reduced by leaving temperatures unconstrained. A higher vertical resolution of 90 levels increases the stratospheric residence time of sulfate aerosol by reducing the diffusion out of the tropical reservoir. We conclude that the model set-up (vertical resolution, free-running vs. nudged) as well as forcing parameters (volcanic emission strength, plume height) contribute equally to the model uncertainties.

Modeling the Sulfate Aerosol Evolution after Recent Moderate Volcanic Activity, 2008-2012

Christina V. Brodowsky[1,2], Timofei Sukhodolov[1,2,3], Aryeh Feinberg[1,4,5], Michael Höpfner[6], Thomas Peter[1], Andrea Stenke[1,4], and Eugene Rozanov[1,2,3]

[1]Institute for Atmospheric and Climate Science, ETH Zürich, Zürich, Switzerland
[2]Physikalisch-Meteorologisches Observatorium Davos and World Radiation Center, Davos, Switzerland
[3]St. Petersburg State University, St. Petersburg, Russia
[4]Institute of Biogeochemistry and Pollutant Dynamics, ETH Zürich, Zürich, Switzerland
[5]Eawag, Swiss Feteral Institute of Aquatic Science and Technology, Dübendorf, Switzerland
[6]Institute of Meteorology and Climate Research, Karlsruhe Institute of Technology, Karlsruhe, Germany

Key Points:

- Differences in estimates for volcanic emissions have a large effect on the aerosol evolution in the model
- Shifts in the tropopause cause variability in free running simulations but nudging leads to side effects and an increased sulfur burden
- An increased vertical resolution changes the diffusion of aerosols out of the tropical reservoir and therefore the lifetime

Corresponding author: Christina Brodowsky, `brodowsc@ethz.ch`

Abstract

Volcanic activity is a main natural climate forcing and an accurate representation of volcanic aerosols in global climate models is essential. This is, however, a complex task involving many uncertainties related to the magnitude and vertical distribution of volcanic emissions as well as in observations used for model evaluation. We analyse the performance of the aerosol-chemistry-climate model SOCOL-AERv2 for three medium-sized volcanic eruptions. We investigate the impact of differences in the volcanic plume height and SO_2 content on the stratospheric aerosol burden. The influence of internal model variability and dynamics are addressed through an ensemble of free-running and nudged simulations at different vertical resolutions. Comparing the modeled evolution of the stratospheric aerosol loading to satellite measurements reveals a good performance of SOCOL-AERv2. However, the large spread in emission estimates leads to differences in the simulated aerosol burdens resulting from uncertainties in total emitted sulfur and the vertical distribution of injections. The tropopause height varies among the free-running simulations, affecting model results. Conclusive model validation is complicated by uncertainties in observations. In nudged mode, changes in convection and tropospheric clouds affect SO_2 oxidation paths and cross-tropopause transport, leading to increased burdens. This effect can be reduced by leaving temperatures unconstrained. A higher vertical resolution of 90 levels increases the stratospheric residence time of sulfate aerosol by reducing the diffusion out of the tropical reservoir. We conclude that the model set-up (vertical resolution, free-running vs. nudged) as well as forcing parameters (volcanic emission strength, plume height) contribute equally to the model uncertainties.

1 Introduction

Volcanic injections of sulfur dioxide into the stratosphere can have significant and sudden effects on the global climate. The best known example is the 1815 Tambora eruption, which one year later led to what we now know as the "year without summer". Though thousands of kilometres away, the consequences of this eruption have been documented in Europe and elsewhere in the world (Raible et al., 2016). The most recent major event was the Pinatubo eruption in 1991. Though less explosive than Tambora by around an order of magnitude, it still had a significant impact on global climate (e.g. McCormick et al., 1995; Trenberth & Dai, 2007). As of the writing of this article, there have not been any major volcanic eruptions since the Pinatubo event. There has, however, been some intermittent volcanic activity since the year 2000, which resulted in a global volcanic aerosol forcing of about -0.19 W/m^2 (Ridley et al., 2014).

During explosive volcanic eruptions, sulfur dioxide (SO_2) can be injected into the stratosphere where it leads to the formation of sulfuric acid aerosol particles. These particles have a lifetime in the stratosphere of up to several years and, in case of equatorial eruptions, are transported polewards on a large scale via the Brewer-Dobson Circulation (BDC) (Kremser et al., 2016). Elevated aerosol levels in the stratosphere have various effects on the climate. They prevent part of the solar radiation from reaching the earth's surface by scattering shortwave radiation back to space (e.g. Andersson et al., 2015). This results in a net cooling of the troposphere. Furthermore, induced changes in the hydrological cycle can for example lead to droughts (Kremser et al., 2016; Timmreck, 2012; Trenberth & Dai, 2007). The cooling effect has inspired potential geoengineering schemes, where sulfur would artificially and continuously be injected into the stratosphere to achieve a counter effect to greenhouse gas-caused warming (e.g. Crutzen, 2006). This, however, comes with a wide range of negative side effects as observed after past volcanic eruptions (e.g. Trenberth & Dai, 2007), apart from ethical and political concerns (MacMartin et al., 2018). Besides cooling the surface, the stratosphere is heated as the sulfate particles absorb the upwelling infrared radiation, which in turn modifies the stratospheric circulation (Diallo et al., 2017). Due to heterogeneous chemical reactions on/in the particles, stratospheric eruptions also affect the chemistry of the atmosphere by altering ozone (O_3) depletion cycles (Revell et al., 2017).

Since the Pinatubo eruption almost 30 years ago, the most notable events have been Kasatochi (2008), Sarychev (2009), Nabro (2011), and Raikoke (2019), each injecting between 1 and 2 Tg of sulfur into the stratosphere (Andersson et al., 2015; S. Carn, 2019; de Leeuw et al., 2020). They are often referred to as medium-sized or even small eruptions in terms of their impact on climate (e.g. Brühl et al., 2015). The 1991 Pinatubo eruption released about ten times more SO_2 than Sarychev or Nabro (S. Carn, 2019). It led to a surface cooling of about 0.5 K, though the exact amount and distribution of SO_2 following this event is still very uncertain (Dutton & Christy, 1992; Sukhodolov et al., 2018), which complicates understanding of the underlying physics. A major volcanic eruption like this can and most likely will happen again. With the means we have today, it is possible to make projections and prepare in order to mitigate societal or political effects (Kremser et al., 2016). For example, the Pinatubo eruption of 1991 resulted in estimated global average crop yield losses in 1992 of ~1% for wheat, ~4% for rice, and ~6% for both maize and soy (Proctor et al., 2018).

Satellite data coverage has improved within the last decades. In the 1990's, the main satellite instruments were SAGE II and HALOE, which documented the Pinatubo eruption with monthly temporal and 1-2 km vertical resolution, whereas nowadays near-daily global data sets with higher vertical resolution are available (Kremser et al., 2016; von Savigny et al., 2020). Modeling studies often focus on the 1991 Pinatubo eruption as it is the largest event since continuous atmospheric observations have become available (Arfeuille et al., 2013). The chemistry climate model SOCOL-AERv1 has also been used to simulate the effects of the Pinatubo event (Sukhodolov et al., 2018). The same time period has been reevaluated by Feinberg et al. (2019) using SOCOL-AERv2 after important updates to the model, e.g. improving sulfate mass conservation. Overall, our previous results showed a reasonable model performance in many aspects, including the ozone response to Pinatubo, although a large uncertainty in the observational data made it difficult to derive the exact conclusions both on the model performance and the atmospheric effects.

A recent sequence of medium-sized events is well covered by observational data from different sources and presents another opportunity for model validation and a study of the volcanic effects in the stratosphere. Volcanic activity in the time period from 2008 to 2012, when the eruptions of Kasatochi, Sarychev and Nabro occured, has been modeled for instance by Günther et al. (2018) to validate SO_2 and sulfate aerosol dataset derived from the Michelson Interferometer for Passive Atmospheric Sounding (MIPAS). Brühl et al. (2015) used the time period from 2002 to 2011 to evaluate the representation of aerosol module of the chemistry-climate model EMAC. Mills et al. (2016) simulated the whole time span from 1990 to 2014 with the Whole Atmosphere Community Climate Model (WACCM), therefore covering both the Pinatubo event as well as more recent volcanic activity. However, like in the Pinatubo case, all previous studies relied on the emission estimates that were specific to their studies and are quite different compared to each other. The reported different levels of the model performances emphasize potential uncertainties in all involved factors, namely, the model's features, the observations used for validation, and the emission estimates, that are also derived from observations. In addition, the models used in those studies relied on lognormal size distributions approximations or other crude size assumptions, i.e. none of them used a sectional aerosol model as in SOCOL-AERv2, which could have potentially important repercussions for aerosol lifetime representations.

The aim of this study, therefore, is to further investigate how our model performs with smaller but more recent volcanic events, but also to address the related modeling uncertainties. This is essential before applying the model to project the impact of future eruptions or potential geoengineering strategies involving stratospheric aerosols. The possibility of a large volcanic eruption led to the implementation of the VolRes initiative, which seeks to understand the climate response to these eruptions better and to develop a fast response plan in case of an event (`https://wiki.earthdata.nasa.gov/display/volres/Volcano+Response`), which also includes modelling in order to predict the po-

tential effects and duration of the event. In this case the model would rely on the emission parameters derived from observations during the eruption, but it would first have to be driven by the observed dynamical fields (specified dynamics or "nudging" mode), which can introduce side effects that also have to be investigated in advance.

In the present work, a closer look is taken at the eruptions of Kasatochi in 2008, Sarychev in 2009 and Nabro in 2011. The model is used to simulate the consequences of volcanic eruptions, namely aerosol formation from the precursor gas SO_2, and its lifetime and transport in the stratosphere. The four main points of interest are (i) the uncertainty in volcanic emissions, (ii) the internal variability of the system, (iii) the difference between nudged and free running simulations, and (iv) the influence of a higher vertical resolution. The latter has been suggested by Sukhodolov et al. (2018) as a potential factor that could improve the aerosol lifetime representation.

Section 2 describes the methods applied, including a brief description of the model and an overview of the observational data sets used for comparison, as well as some background information about the time period that was used for this model validation. Section 3 presents the simulation results, which are discussed in relation to the observations and referring to the four main assessment points mentioned above. Summarizing conclusions are provided in Section 4.

2 Methods

2.1 Model Description

SOCOL-AERv2 is a coupled aerosol-chemistry-climate model (Feinberg et al., 2019; Sheng et al., 2015). The chemistry-climate part SOCOL consists of the global circulation model MA-ECHAM5 coupled to the chemistry module MEZON (Stenke et al., 2013). The third component, AER, is a sectional aerosol model, which describes the sulfate aerosol microphysics and chemistry. The latter is integrated into MEZON (Sheng et al., 2015). A list of all relevant reactions of the sulphur chemistry is given by Sheng et al. (2015). SOCOL-AERv2 is an updated version of SOCOL-AERv1 (Feinberg et al., 2019). The new features include an update of reaction coefficients, a switch from wet to dry radius for microphysical calculations (with improved mass conservation), and the addition of interactive deposition schemes. The aerosol in SOCOL-AERv2 is divided in 40 size bins with dry radii (i.e. pure H_2SO_4) for microphysical calculations in the model. These radii range from 0.39 nm to 3.2 μm, corresponding to nominally 2.8 molecules of H_2SO_4 for the smallest and 1.6×10^{12} molecules for the largest particle, with molecule numbers doubling between neighbouring bins (Feinberg et al., 2019). The default volcanic forcing data is taken from a database by S. A. Carn et al. (2016). The initial volcanic plume is prescribed as an vertically uniform distribution of the SO_2 extending from the top of the plume and downwards one third of the way to the earth's surface in a single grid box, as recommended by Diehl et al. (2012) (and personal communication with S. Carn). The SO_2 emission due to continuous volcanic degassing is horizontally distributed according to volcano locations and set to 12.6 Tg S yr^{-1} based on the data set of Andres and Kasgnoc (1998) with suggested corrections (Dentener et al., 2006). Other SO_2 surface emissions include anthropogenic and biomass burning sources, which are taken from the MACCCITY inventory (Granier et al., 2011). DMS fluxes are calculated online using a wind-driven parametrization (Nightingale et al., 2000) and a climatology of sea surface DMS concentrations (Kettle et al., 1999; Kettle & Andreae, 2000). 1 Tg S yr^{-1} of CS_2 is emitted between the latitudes of 52°S and 52°N. The mixing ratios of H_2S and OCS are fixed at the surface to 30 pptv (Weisenstein et al., 1997) and 510 pptv (Montzka et al., 2007), respectively. A detailed description of the model, its other standard boundary conditions, and recent upgrades is given in Feinberg et al. (2019). However, in that study the main focus was on deposition fluxes and stratospheric processes and only non-volcanic conditions were considered.

In the present work we use SOCOL with prescribed sea surface temperatures (SSTs) and sea ice coverage (SIC). For ocean-coupled versions of SOCOLv3 see for example Muthers et al. (2014), or refer to the new SOCOLv4 introduced by Sukhodolov et al. (2021). SSTs and SIC are prescribed using observations from the Hadley Centre (Rayner et al., 2003). The model can either be used in free running or in specified dynamics (nudged) modes. Nudging means that wind and temperature fields generated by the model are continuously corrected towards meteorological reanalysis data (Zhang et al., 2014). In SOCOL-AERv2, vorticity and divergence of the wind fields, temperature and surface level pressure can be nudged to ERA-Interim reanalysis (Dee et al., 2011). SOCOL-AERv2 by default runs on 39 hybrid vertical levels, but the vertical resolution can be increased to 90 levels (Stenke et al., 2013). Since the default 39 vertical levels are insufficient to generate a Quasi Biennial Oscillation (QBO) in free-running mode, the zonal winds in the equatorial stratosphere are nudged to observed wind profiles (Stenke et al., 2013). In this study a model configuration with 39 vertical levels was used in all simulations except for the last experiments, where a sensitivity test was performed applying 90 levels set-up. The horizontal resolution was set to a T42 grid (around $2.8° \times 2.8°$) throughout.

2.2 Observational Datasets

Three data sets were used to validate the model. The SAGE-3λ stratospheric aerosol dataset from phase 6 of the Coupled Model Intercomparison Project (CMIP6 Eyring et al., 2016) is a composite of satellite observations combined with the AER-2D model. In the period of 2008 to 2012 specifically, monthly mean data from the Optical Spectrograph and InfraRed Imager System (OSIRIS) and the nadir viewing Cloud-Aerosol Lidar and Infrared Pathfinder Satellite Observation (CALIPSO) were used (Thomason et al., 2018). A brief overview of this data set is given in (Revell et al., 2017).

Additionally, two level 3 data sets derived from the Michelson Interferometer for Passive Atmospheric sounding (MIPAS) for SO_2 (Höpfner et al., 2015) and sulfate aerosol (Günther et al., 2018) were used. The infrared limb emission sounder MIPAS was an instrument on board Envisat covering the period between 2002 and 2012. Regarding the MIPAS data of SO_2, comparisons with independent observations showed typical biases within ± 50 pptv. Sampling artifacts due to pre-filtering of MIPAS limb-scans with large ash and aerosol contribution as well as saturation effects in the limb-spectra lead to an underestimation of the total SO_2 mass derived from all remaining profiles a few weeks after larger volcanic eruptions like Sarychev. The MIPAS data set of aerosol volume density profiles is based on the assumption that all particles consist of liquid sulfuric acid with 75 wt% H_2SO_4. Note that the originally retrieved aerosol volume densities from MIPAS were adjusted globally by an altitude dependent negative offset based on comparisons with in situ data from Laramie, Wyoming. Further, filters on cirrus, ash and PSCs were applied (Günther et al., 2018).

2.3 Experimental Setup

Since the 1991 Pinatubo eruption, there have not been any similarly large volcanic events. Especially between the years 2000 and 2005 there was very little distinguishable influence on the climate system by explosive volcanic activity. After this time period, there have been a few notable events with measurable impact on global climate, albeit much smaller than the Pinatubo eruption. These eruptions have also been observed by remote sensing instruments, such as MIPAS and CALIOP (Cloud-Aerosol Lidar with Orthogonal Polarization). Therefore, we concentrate on the time period from 2008 to 2012, since three events (Kasatochi in 2008, Sarychev in 2009 and Nabro in 2011) were close in time, and they were all stratospheric and injected a relatively large amount of SO_2 of more than 1 Tg (estimates for emissions are discussed in section 2.3.1). In the troposphere, SO_2 typically has a chemical lifetime of a few days to weeks. This is due to quick removal via fast aqueous phase oxidation and subsequent scavenging and precip-

itation. In the stratosphere, less oxidizing agents are available, therefore SO_2 can last for several weeks before being converted to sulfuric acid, H_2SO_4 (Kremser et al., 2016). Since there is also no wet removal, the stratospheric aerosol can last for several months or even years in the case of events the size of Pinatubo (Trenberth & Dai, 2007). The particles leave the stratosphere via gravitational sedimentation or transport through tropopause folds to the troposphere as well as subsidence at high latitudes (McCormick et al., 1995; Kremser et al., 2016; Timmreck et al., 2018).

Both the latitude and season of the eruption impact the transport to the other hemisphere (Butchart, 2014; Swingedouw et al., 2017; Timmreck et al., 2018; Toohey et al., 2011). For eruptions in the winter hemisphere, there is an increased transport towards the winter pole, whereas there is a higher probability of stratospheric transport from the summer towards the winter hemisphere, which is, however, also dependent on the altitude of the SO_2 emission as there are upper and lower branches of the Brewer Dobson Circulation (BDC) with their specific transport routes and seasonalities (Konopka et al., 2015). All considered events occurred during the summer months. Kasatochi and Sarychev are located far North (52°N and 48°N), while Nabro can be considered tropical (13°N). These events are discussed in more detail in the next section.

The list of performed modeling experiments is presented in Table 1 and the four main topics we are addressing are described in the following sections.

Table 1. All performed simulations with their respective set-up for this study concerning nudging, the volcanic emission database as well as the vertical resolution. *Free1-3* are three free running members of an ensemble simulation.

Simulation	Nudged Parameters	Vertical Resolution	Volcanic Emission Database		
			Name	Satellite instruments	References
NdgDB1	u, v, T	39	VolcDB1	MIPAS and GOMOS	Bingen et al. (2017); Brühl (2018)
NdgDB2	u, v, T	39	VolcDB2	UV, IR, m-wave satellite instruments	Neely and Schmidt (2016); Mills et al. (2016)
NdgWT	u, v, T	39	VolcDB3	UV, IR, m-wave satellite instruments	S. Carn (2019)
NdgDB4	u, v, T	39	VolcDB4	TOMS and OMI	Diehl et al. (2012)
Volc0	u, v, T	39	None		
Free1-3	None	39	VolcDB3		
NdgW	u, v	39	VolcDB3	see above	see above
NdgW90	u, v	90	VolcDB3		
NdgIdeal39	u, v	39	None[a]		
NdgIdeal90	u, v	90	None[a]		

[a] Emissions for a single volcanic event were prescribed separately.

2.3.1 Databases for Volcanic SO_2 Emissions

The modeling of volcanic aerosol faces many uncertainties, including size distribution, microphysics and meridional transport. This is affected by the model's properties but also to a large extent by vertical extent and SO_2 amount in the initial volcanic plume (Timmreck et al., 2018). The Interactive Stratospheric Aerosol Model Intercomparison Project (ISA-MIP) seeks to reduce such uncertainties and proposes a set of experiments to be done with different global climate models with interactive sulfur chemistry and stratospheric aerosol (Timmreck et al., 2018). This study uses the set-up of five of the Transient Aerosol Record (TAR) experiments described in Timmreck et al. (2018), however, only for the limited timespan from 2008 to 2012 (instead of 1998 - 2012). The aim is to investigate the consequences of using a diverse set of inventories for volcanic eruptive SO_2 emissions on stratospheric aerosol. Details about volcanic emissions from four databases are presented in Table 2.

Timmreck et al. (2018) recommend four databases as volcanic forcing data in climate models. In the following they are referred to as VolcDB1 - VolcDB4. These databases provide SO_2 emissions from volcanic eruptions as well as the plume top height after an event. The VolcDB1 database (Bingen et al., 2017; Brühl, 2018) is compiled from observations by the Envisat instruments MIPAS and GOMOS (Global Ozone Monitoring

Table 2. A list of the most important volcanic events that happened between 2005 and 2015. All events emitted at least 0.1 Tg of SO_2 and had an initial plume that likely reached the stratosphere are included. The eruptions of Kasatochi, Sarychev and Nabro shown in boldface most likely resulted in the largest aerosol production and are analyzed in this study. Out of the four databases, only VolcDB2 provides the vertical extent of the volcanic plumes. For the other three databases, the emitted SO_2 plume is assumed to be evenly distributed the given plume top downwards one third of the way to the earth's surface.

		VolcDB1		VolcDB2		VolcDB3		VolcDB4	
Volcano	**Date**	**SO_2 (Tg)**	**Plume (km)**	**SO_2 (Tg)**	**Plume (km)**	**SO_2 (Tg)**	**Plume (km)**	**SO_2 (Tg)**	**Plume (km)**
Sierra Negra	22 Oct 2005			0.36	14 - 15				
0.83° S, 91.17° W	23 Oct 2005					0.28	15	1.00	6
	24 Oct 2005					0.57	5		
	25 Oct 2005	0.02	15			0.22	5		
	26 Oct 2005					0.52	5		
	28 Oct 2005					0.24	5		
	29 Oct 2005					0.10	2		
Soufrière Hills	19 May 2006			0.20	19 - 20				
16.72° N, 62.18° W	20 May 2006					0.20	20	0.14	16.8
	23 May 2006	0.16	19						
Rabaul	7 Oct 2006			0.23	17 - 18	0.30	18	0.23	18
4.27° S, 152.20° E	10 Oct 2006	0.17	17						
Nyamuragira	27 Nov 2006					0.14	15		
1.41°S, 29.2° E	28 Nov 2006			0.20	3 - 9	0.16	14	0.22	4.5
	29 Nov 2006	0.04	17	0.47	3 - 8	0.25	9	0.32	4.5
	30 Nov 2006			0.68	3 - 8	0.04	14	0.30	4.5
	1 Dec 2006			0.69	3 - 8	0.06	10	0.10	4.5
	2 Dec 2006			0.61	3 - 8	0.01	8		
	3 Dec 2006					0.01	5		
Okmok	12 Jul 2008			0.12	10 - 16	0.15	15	0.04	15.2
53.42° N, 168.13° W	13 Jul 2008							0.06	13.7
	14 Jul 2008							0.03	9
	21 Jul 2008	0.06	16						
Kasatochi	7 Aug 2008					2.00	15		
52.18° N, 175.51° W	8 Aug 2008			1.70	10 - 18			1.70	12.5
	15 Aug 2008	0.39	17						
Alu-Dalafilla	3 Nov 2008					0.15	16		
13.82° N, 40.55° E	13 Nov 2008	0.06	17						
Sarychev	12 Jun 2009							0.93	16
48.09° N, 153.20° E	13 Jun 2009							0.02	12
	14 Jun 2009							0.16	12
	15 Jun 2009			0.60	11 - 15	1.20	17	0.06	12
	16 Jun 2009			0.60	11 - 15			0.44	9.7
	17 Jun 2009							0.36	3[a]
	21 Jun 2009	0.50	16						
Merapi	4 Nov 2010					0.30	17		
7.54° S, 110.44° E	8 Nov 2010	0.11	17	0.44	14 - 15.2				
Cordón Caulle	4 Jun 2011			0.25	12 - 13.7	0.20	14		
40.59° S, 72.12° W	11 Jun 2011	0.02	13						
Nabro	13 Jun 2011			1.50	9.7 - 17	0.62	18		
13.37 ° N, 41.70° E	14 Jun 2011			0.51	2.5 - 7.8	0.16	18		
	15 Jun 2011			0.74	2.5 - 6.8	0.70	18		
	16 Jun 2011			0.57	2.5 - 9.2	0.43	18		
	17 Jun 2011			0.20	2.5 - 9.5	0.20	6		
	18 Jun 2011			0.20	2.5 - 6.7	0.20	6		
	19 Jun 2011			0.23	2.5 - 6.5	0.10	6		
	20 Jun 2011			0.24	2.5 - 5.2	0.12	6		
	21 Jun 2011	0.45	18	0.23	2.5 - 5.2	0.07	6		
	22 Jun 2011			0.16	2.5 - 5.7	0.14	6		
	23 Jun 2011			0.11	2.5 - 5.9	0.03	6		
	24 Jun 2011			0.01	2.5 - 6.2	0.07	6		
	25 Jun 2011			0.11	2.5 - 5.1	0.02	6		
	26 Jun 2011			0.13	2.5 - 4.6	0.18	6		
	27 Jun 2011			0.07	2.5 - 4.7	0.09	6		
	28 Jun 2011			0.07	2.5 - 6	0.03	6[b]		
Kelut	13 Feb 2014			0.30	17 - 26	0.20	19		
7.93° S, 112.31° E									
Sangeang Api	30 May 2014			0.10	13.7 - 15.2	0.10	17		
8.18° S, 119.06° E									
Calbuco	22 Apr 2015					0.40	20		
41.33°S, 72.62° W									

[a] Minor activity continues with a plume height up to 3km until 27. Jun 2009
[b] Activity continues until 26. Jul, leading to further emissions between 0.006 and 0.047 Tg, sometimes at altitudes up to 26km (S. Carn, 2019) .

by Occultation of Stars). Specifically the SO_2 dataset described in Höpfner et al. (2015) was used. To overcome data gaps resulting from the sampling of fresh volcanic plumes (which may become opaque) and other data gaps, the dataset exploits 5-day averaged distributions (Brühl et al., 2015). This is why the dates of the eruptions deviate slightly from the other databases in Table 2. VolcDB2 (Mills et al., 2016; Neely & Schmidt, 2016) is a compilation of data from several online sources and previously published estimates derived from various satellite observations. It is the only one that provides the minimal plume height as well as the plume top height. VolcDB3 (S. Carn, 2019) is derived from multiple satellite sensors using different measuring techniques (S. A. Carn et al., 2016). The VolcDB3 database is the default for volcanic eruptive emissions in SOCOL-AERv2 following Feinberg et al. (2019), since it is the most detailed database and is continuously updated. While VolcDB2 and VolcDB3 include stratospheric and tropospheric emissions, VolcDB1 only includes the stratospheric part of the SO_2 emissions. VolcDB4 (Diehl et al., 2012, `https://aerocom.met.no/DATA/download/emissions/HTAP/`) is compiled from TOMS and OMI satellite data as well as additional data from the Global volcanism program; however, being an older database, it only covers a time period until 2010 (Timmreck et al., 2018).

The various instruments and methods to retrieve and validate these datasets lead to sometimes rather large differences in the estimated SO_2 emission as well as the height of the original volcanic plume, as can be seen in Table 2. In many cases it is uncertain how much of the eruptive material reaches higher altitudes (von Savigny et al., 2020).

Kasatochi is a volcano on the Aleutian Islands, USA, at 52°N, which erupted in August 2008. The amount of sulfur emitted into the stratosphere ranges from 0.39 Tg in VolcDB1 to 2 Tg in VolcDB3. The height of the plume is estimated between 12.5 and 18 km. Sarychev, a volcano on the Kuril Islands, Russia, at 48°N, erupted in June 2009. Between 0.5 Tg SO_2 according to VolcDB1 and 1.2 Tg of SO_2 in VolcDB3 and VolcDB2 were emitted into the stratosphere. The maximum height of the plume was estimated to be between 15 to 16 km, see Table 2. Nabro in Eritrea, at 13°N, is the closest to the equator of the three eruptions. The eruption started on 13 June 2011, lasting for weeks. The plume reached the stratosphere mainly during the first few days (Clarisse et al., 2014). The estimates for SO_2 emissions range from 0.446 Tg in VolcDB1 to 1.9 Tg in VolcDB3 with a maximal plume height of 17 to 18 km. Several more eruptions took place during this time period that are listed in Table 2. However, these eruptions are not analyzed in detail here as their emissions are much lower and a pronounced effect on the climate has not been reported. Their SO_2 input into the atmosphere is still considered in the model as it contributes to the background sulfur burden. Note that not all of these minor events are present in all four databases, which also affects the resulting modelling differences.

Four nudged simulations (*NdgDB1/2/4* and *NdgWT*) were done, each with one of the databases DB1-4, and another simulation was carried out without explosive volcanic emissions (however, with volcanic degassing, *Volc0*) in order to demonstrate the contribution of stratospheric eruptions to the aerosol layer evolution. *NdgWT* uses VolcDB3 (see Table 1) but has a special name, since it is widely used throughout all analysis sections.

2.3.2 Internal Variability

The next point of interest was the internal variability of the model itself. The natural system can never be perfectly described by any model as both the initial and boundary conditions have a certain error margin and the treatment of different processes by the model is simplified relative to the real world. Model outputs therefore depend on both the characteristics of the model but are also sensitive to the background state of the atmospheric system (Timmreck, 2012; Zanchettin et al., 2016). The randomness which ensues is depicted using an ensemble of simulations with slightly different boundary conditions (here depicted by a tiny perturbation of the initial CO_2 concentration). In this

case, three such ensemble members were used (hereafter called *Free1*, *Free2* and *Free3* or simply *Free* for all three ensemble members).

2.3.3 Free vs. Nudged

To avoid this variability and to ensure best possible comparability with measurements, the model's dynamics can be nudged towards observations (Zhang et al., 2014). In this third test, two more simulations were run with the same set up as the first ensemble member but once nudged to observed temperature and wind fields (hereafter called *NdgWT*) and the other nudged to only wind fields (*NdgW*). The objective was to find out how nudging affects SOCOL-AERv2 and if it improves performance or leads to other side effects. Should the model be used for forecasting or nowcasting, it would be run in nudged mode to set the stage for the eruption, after which the model would be switched to free running mode. There might be some undesired side effects from switching between nudged and free-running mode that have an effect on the simulation of the volcanic aerosol and the climate response, that we wanted to investigate.

2.3.4 Increased Vertical Resolution

In a previous study with SOCOL-AERv2 about the Pinatubo eruption, it was suggested that the vertical resolution affects the aerosol lifetime (Sukhodolov et al., 2018). At the time, the model was run with a vertical resolution of 39 levels; it can however be increased to 90 levels (Stenke et al., 2013). The set up with 90 vertical levels was used for the same time period from 2008 to 2012 to see if it would improve the model performance. In this context, another simulation analogous to *NdgW* was done, which is hereafter called *NdgW90*. Additionally, idealized simulations were run in both vertical resolutions (*NdgIdeal39* and *NdgIdeal90*), in which a single volcanic event was prescribed, whereas all other volcanic emissions were turned off in order to isolate the signal from this single event. Note that, although the 90-level version is able to generate a realistic QBO, we kept it prescribed in the same way as in the 39-level version for the sake of consistency.

3 Results and Discussion

3.1 Databases for Volcanic SO_2

In order to evaluate and improve climate models, reliable databases and observations are essential (Bingen et al., 2017; Zanchettin et al., 2016). Despite continuously improving measurement techniques, the exact parameters of volcanic eruptions are still not perfectly clear (von Savigny et al., 2020). In a first step, we evaluate the impact of the volcanic SO_2 emission data on the simulated aerosol distribution by comparing a set of nudged model simulations using the four databases VolcBD1 to VolcBD4 to show the uncertainty related to the data retrieval after volcanic events.

Figure 1 shows sulfur burdens for the stratosphere (a) and the entire atmosphere (b) for the four simulations *NdgDB1/2/4* and *NdgWT* as well as for one simulation without the eruptive emissions but only time-independent volcanic SO_2 degassing (*Volc0*), which is identical in all model simulations. The difference between *Volc0* and the other simulations directly demonstrates the impact of volcanic eruptions on the stratospheric and total sulfur burden. We note that *Volc0* shows a clear seasonal cycle with maximum loads in boreal fall and minima in spring. This is caused mainly by the seasonal variability in the tropospheric oxidation capacity, converting SO_2 and OCS more effectively to H_2SO_4 in summer and fall (Graf et al., 1998) and by the seasonality of anthropogenic and dimethyl sulfide (DMS) emission. In addition, there is interannual variability in the total aerosol in Figure 1b, which can be attributed to the variability in washout processes and transient non-volcanic sulfur sources. Most of the differences in total sulfur in Fig-

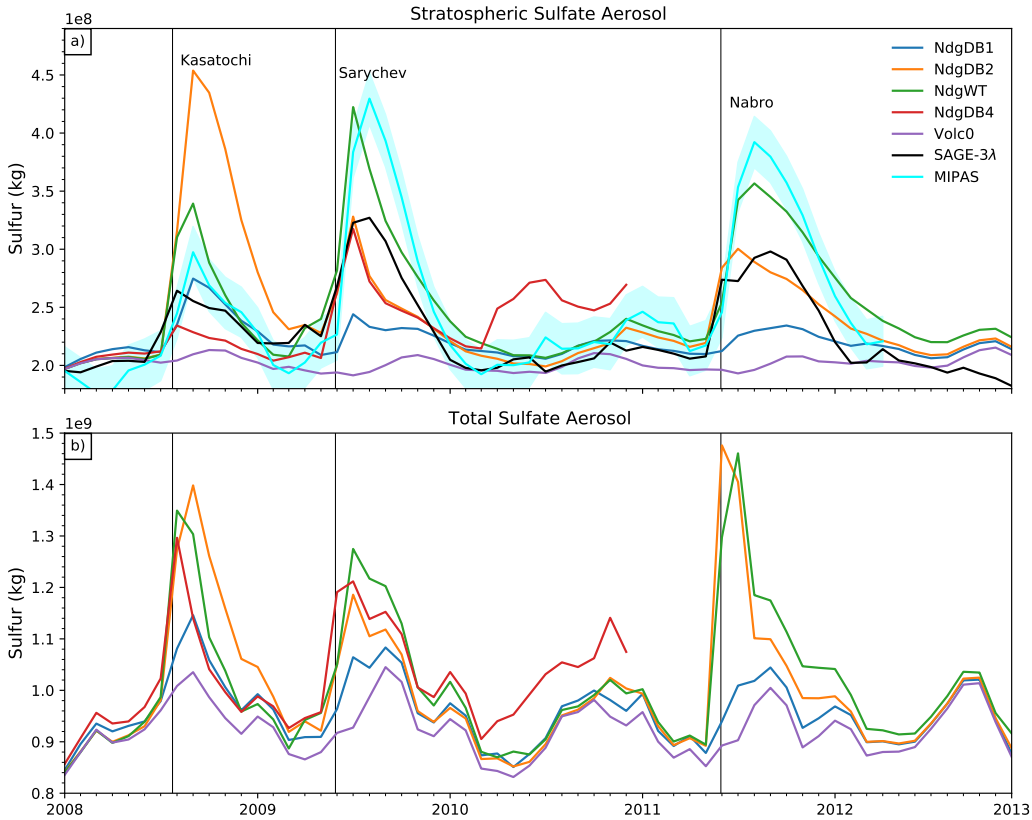

Figure 1. (a) Evolution of the global, monthly mean total stratospheric aerosol burden [10^8 kg S], simulated with SOCOL-AERv2, using the VolcDB1-4 databases (*NdgWT* uses VolcDB3) and nudged to observed winds and temperatures in comparison with the SAGE-3λ and MIPAS aerosol datasets. The MIPAS data is corrected for baseline differences with a constant value and the tropopause for SAGE-3λ and MIPAS is taken from ERA-Interim reanalysis. (b) Same as (a) but for the total atmospheric burden of sulfate aerosol [10^9 kg S]. Observations are only included in the stratosphere due to lacking tropospheric data. The three main peaks indicate elevated sulfate aerosol levels after the eruptions of Kasatochi in 2008, Sarychev in 2009 and Nabro in 2011.

ure 1b can be attributed to differences in the estimated amount of the initial emission listed in Table 2. It is expected that *NdgDB1* would show a smaller sulfur loading during volcanically enhanced periods, as VolcDB1 has the lowest estimates for SO_2 emissions due to the fact that only stratospheric emissions are considered. Therefore potential upwards transport of volcanic SO_2 from the troposphere into the stratosphere does not contribute to the stratospheric burden.

The differences in stratospheric sulfur in Figure 1a between the simulations for the different databases depend on the height of the initial volcanic plume with respect to the tropopause. In these four simulations the tropopause position had been defined by the nudging procedure and therefore did not vary among the four realizations. The deciding factor is therefore the height and the vertical distribution of the volcanic plume that influences the percentage of sulfur which reaches the stratosphere.

For Kasatochi in 2008, we see a much higher peak for *NdgWT* (VolcDB3) and for *NdgDB2* (VolcDB2) in Figure 1b. The total sulfur column for *NdgWT* in this case is al-

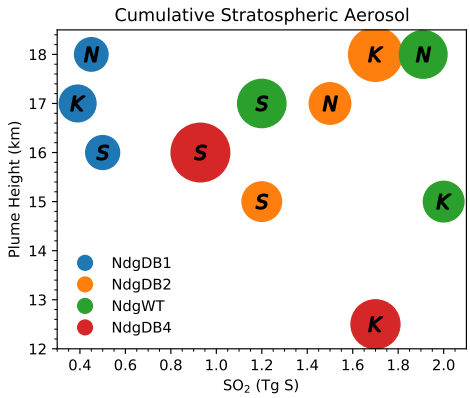

Figure 2. The stratospheric sulfate aerosol, added up over 6 months for *NdgDB1/2/4* and *NdgWT*. Each circle stands for one of the three main eruptions; Kasatochi (K), Sarychev (S) or Nabro (N), where the size is relative to the cumulative amount of aerosol as a function of initial plume top height and SO_2 content.

most three times higher than the one for *NdgDB1* (VolcDB1) disregarding the background of about 0.9×10^9 kg sulfur. VolcDB1 often has the lowest values for volcanic SO_2, as can be seen in Table 2, which naturally leads to the lowest sulfur load as confirmed by SOCOL-AERv2. In the model results, these low emission values hardly overcome internal tropospheric variability. This is also illustrated in Figure 2, where the size of the circles represents the cumulative sulfate aerosol over the course of six months as a function of emission height and emitted SO_2. *NdgDB1* clearly has the lowest initial SO_2 emissions and even though the plume height was relatively high, the cumulative stratospheric aerosol remained low compared to *NdgDB2* and *NdgDB3*. The second main peak in Figure 1, which corresponds to the 2009 Sarychev eruption, exhibits a similar temporal extension as the one for Kasatochi. The third peak represents the 2011 Nabro eruption, which differs in the duration of the eruption as archived in the four databases. The Nabro eruption was very complex as it lasted for several weeks and sources disagree on how much of the initially emitted SO_2 was directly injected into the stratosphere (Theys et al., 2013). In VolcDB3 the emissions from this eruption are documented as most prolonged. In VolcDB2 the temporal extent of emissions was also picked up, whereas in VolcDB1 all eruptions are described as one-day events. However, it is hard to judge on the importance of this factor, as amplitude and height of the emissions are very different among the databases. For the VolcDB4 database, there is no comparison as it has not been updated for eruptions after 2010. Its significantly higher burden in 2010 is most likely an artefact caused by an overestimated plume height of 16 km for the 2010 Eyjafjallajökull eruption compared to 9 km reported in most other databases. In Figure 2, similarly to *NdgDB1*, *NdgDB4* has rather low cumulative aerosol loadings for both eruptions. In contrast to *NdgDB1*, this is due to the low emission altitude, which illustrates the importance of both factors. A conclusive statement as of the relative importance of these factors is, however, difficult, since only three eruptions were considered and other factors such as the latitude and atmospheric state also contribute.

Figures 1 and 2 illustrate the impact of the large uncertainties concerning volcanic emissions, which ISA-MIP (Timmreck et al., 2018) seeks to reduce. With the current configuration in SOCOL-AERv2, VolcDB3 (*NdgWT*) leads to the closest match with observations from MIPAS. *NdgWT* is also in good agreement with SAGE-3λ, except for the Nabro event, where *NdgDB2* performs best. The lowest values are clearly seen in *NdgDB1*. The VolcDB1 database was also used for model evaluation with the chemistry climate

model EMAC based on ECHAM5, the same dynamical core as in SOCOL-AERv2 (though still different chemistry and aerosol modules) but run on 90 vertical levels and showed a good agreement with observations (Brühl et al., 2015).

3.2 Internal Variability

In this section we explore the impact of model internal variability on the stratospheric sulfur loading by comparing three free running model simulations using the volcanic emission data set VolcDB3 (Fig. 3). For the Kasatochi eruption in 2008, but also for Sarychev in 2009, the three ensemble members develop a large spread, whereas the stratospheric sulfur loading for Nabro is very similar in all three cases. The differences

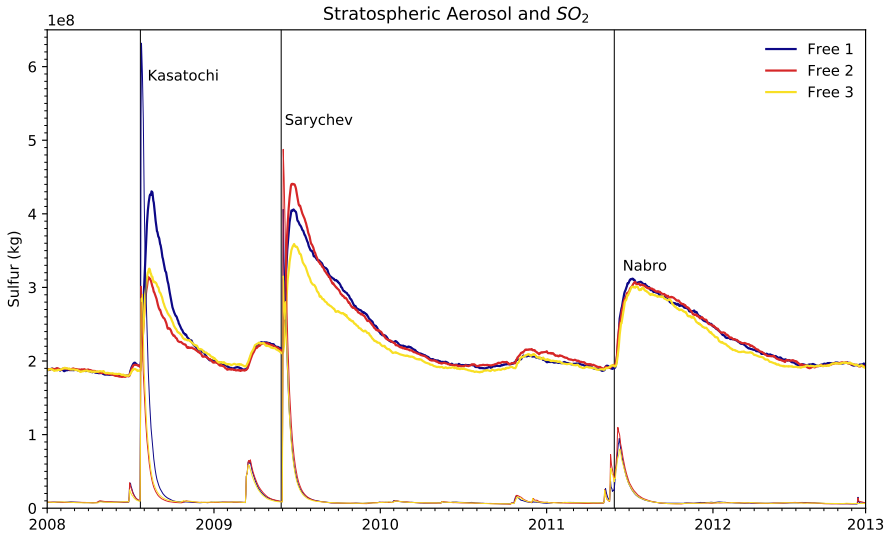

Figure 3. The evolution of the global stratospheric SO_2 (thinner lines) and sulfate aerosol (solid lines) burden [10^8 kg S] for the three free running ensemble members simulated with SOCOL-AERv2 as daily means.

are mainly caused by variations in the tropopause. The volcanic SO_2 injection profiles are the same in all three ensemble members: the emitted SO_2 is evenly distributed within the upper third of the altitude range between plume top and top of the volcano. This means that if the tropopause is lower relative to the volcanic plume, more SO_2 is directly emitted into the stratosphere, which leads to a higher peak aerosol burden as seen for the Kasatochi eruption in *Free1*. While the tropical tropopause height does not undergo large day-to-day changes, the extratropical tropopause height is highly variable. This explains the larger ensemble spread for the two extratropical eruptions of Kasatochi (52°N) and Sarychev (48°N) compared to Nabro, which is located at 13°N.

In view of this sensitivity, we further investigated the role of the tropopause characteristics and the percentage of sulfur reaching altitudes above the tropopause in our simulations, taking account of uncertainties related to the coarseness of the plume profile and from the pressure/altitude conversions using the barometric height formula. In the case of Kasatochi, the tropopause is about 1 km lower for the first ensemble member (11.89 km) in comparison to the other two, which explains its much higher modeled SO_2 and sulfate peaks. In turn, the tropopause for the other two ensemble members is

very similar, at 13.17 km for *Free2* and 12.96 km for *Free3*, explaining the lowest stratospheric sulfur in *Free2*. Considering that the initial volcanic SO_2 injection in the model was assumed to be an event ranging from 10 km to 14 km, the 1-km difference has a significant impact. For the Sarychev eruption the pattern is similar. While the sulfur was injected between 11 km and 16 km and with respective tropopause levels at 11.8 km, 10.69 km and 13.51 km, most of the SO_2 is stratospheric in all three cases. As expected, the sulfur load is again lower for *Free3* with the highest tropopause, as seen in Figure 3. In contrast, for Nabro all three ensemble members keep most of the SO_2 in the troposphere. The modeled tropical tropopause is stable at 17'535 ± 65 m. However, as the volcanic plume reached between 12 km and 18 km, only a small fraction of the SO_2 was directly injected into the stratosphere, which could potentially make a change in tropopause height of only 100 m important. It has been discussed, whether overshooting into the stratosphere was prevalent in case of Nabro, a view corroborated by satellite observations (Vernier et al., 2013; Fromm et al., 2013; Theys et al., 2013; Clarisse et al., 2014, and references therein), or rather an injection into the upper troposphere with subsequent deep convection. In our case, most of the mass was released into the upper troposphere and the model shows good agreement with observations (Figure 1). The fact that all ensemble members in Figure 3 are hardly different for Nabro also suggests that in the model, not only was the tropopause very stable, but also the troposphere to stratosphere flux was strongly pronounced in all ensemble members.

The e-folding times of the sulfate aerosols differ considerably between the three volcanoes, namely ~1.6 months for Kasatochi, ~3.8 months for Sarychev, and ~5.7 months for Nabro. However, for a single volcano the e-folding times are very similar between the three ensemble members (± 15 %).

Finally, it needs to be noted that the tropopause in SOCOL-AERv2 in the free running mode, similar to other chemistry-climate models, shows some bias, especially at higher latitudes, where most models show a too high tropopause compared to reanalysis data (Gettelman et al., 2010). The variability in the extratropical tropopause naturally leads to more uncertainty in modeling. Either the uncertainty can be made visible, as was done here with an ensemble of simulations. Or the model can be nudged, as we show in the next experiment. Another option would be to parametrize the initial volcanic plume profile relative to the tropopause in future studies instead of using the absolute height from the earth's surface.

3.3 Free vs. Nudged

3.3.1 Global Burden

The specified dynamics setup (nudging) in the models is useful for excluding the internal variability and biases in dynamics in order to focus on other processes like chemistry (e.g. Sukhodolov et al., 2018) and also for driving the model by the observed fields with subsequent release to a free-running mode for nowcasting. However, nudging can also introduce artifacts, as the whole system is affected and there are many parameterized subgrid processes that are dependent on the modified global variables. Such artifacts have been already discussed in literature, e.g., in the context of stratospheric transport (Chrysanthou et al., 2019) or cloud effects (Zhang et al., 2014). To explore the potential of SOCOL-AERv2 to be used for nowcasting the plume and effects of the next major eruption, we wanted to analyze such artifacts in relation to the sulfur cycle.

Figure 4 illustrates observations and simulation results in the nudged and free-running modes of the stratospheric and total sulfate aerosol burden. The MIPAS aerosol data set and the SAGE-3λ stratospheric burdens were calculated by applying a tropopause derived from ERA-Interim reanalysis temperature profiles. While the aerosol baseline in the free running model and the *NdgW* simulations and the SAGE-3λ were directly in good agreement without any further adaptation, the *NdgWT* burden showed a higher baseline in aerosol throughout the whole time period. The MIPAS dataset on the other hand shows a lower stratospheric sulfur burden than the simulations or SAGE-3λ, as is

shown in Figure 4b. In order to take account of these discrepancies, we subtract the values of the first month of each observational dataset as well as from each simulated time series, see Figure 4a.

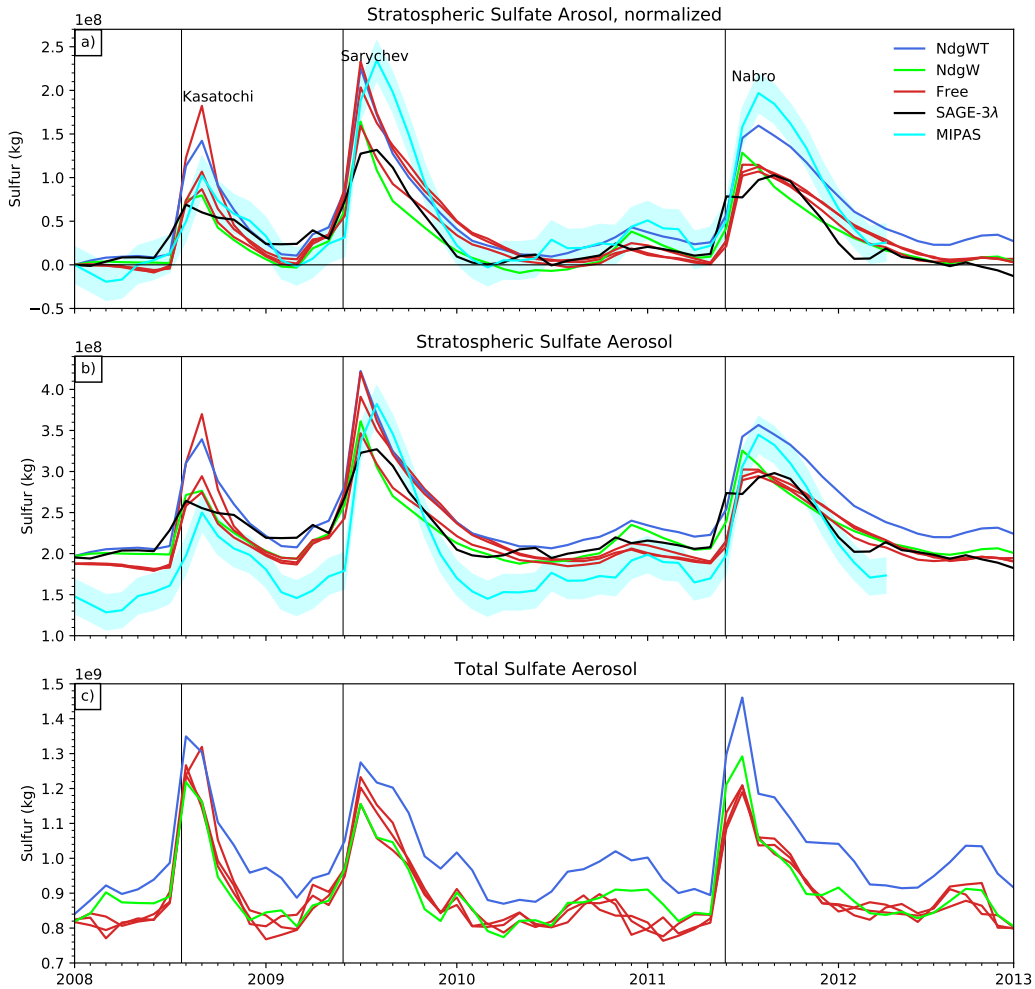

Figure 4. (a) The stratospheric aerosol sulfur burden for *NdgWT*, *Free* and the MIPAS and SAGE-3λ datasets, the value of the first month of each simulation or observation has been subtracted to minimize baseline differences. Shading area around the MIPAS data marks the estimated aerosol retrieval errors (see Günther et al., 2018). (b) The stratospheric aerosol burden without baseline normalization. (c) The total sulfate aerosol in the atmosphere in monthly means for the three free running and the *NdgWT* and *NdgW* simulations.

As seen in Figure 4a, the *NdgWT* simulation is well within the ensemble spread of the Free simulations for the first two events. For Nabro however, the peak is much enhanced for *NdWT*. This may be due to changes in the tropical tropopause layer or tropical deep convection; this is also discussed as a point later in this section about the baseline differences.

The SAGE-3λ dataset is in good agreement with *Free1-3* and *NdgW* for the most part, though it is at the lower end of the ensemble range. MIPAS on the other hand suggests much higher peaks, although still close to the free running ensemble for the first two events. Again it is very interesting that the extremely high peak for the Nabro erup-

tion observed by MIPAS is closer to *NdgWT*. While it is unclear which one is closer to reality in aerosol loading, the e-folding times of stratospheric sulfate aerosol of *Free1-3* and *NdgWT* are in good agreement.

Several factors contribute to the differences in the baseline, shown in figure 4b. First of all, the WMO-defined tropopause calculated from ERA-Interim reanalysis that was applied to SAGE-3λ and MIPAS potentially leads to a low bias, since due to the resolution of these two datasets (500m and 1km respectively) and the ERA-Interim data, there could be cases when the lowermost part of the lower stratosphere is excluded. However, the higher aerosol burden in *NdgWT* is likely due to more complex differences in the model dynamics, particularly affecting cloud formation. The effect on clouds was already described by Jeuken et al. (1996) who showed that particularly the temperature nudging led to a decrease in precipitation in ECHAM. It is also described in more detail in Zhang et al. (2014), who suggest nudging only horizontal wind fields but not temperature as a potential way to mitigate such effects. However, they did not investigate how this might affect aerosols. In comparison, *NdgW* shows much better agreement with *Free1-3* than *NdgWT*. This comes, however, with the cost of having a less constrained model, such that the tropopause effects as described in the previous section become again somewhat more prevalent.

In Figure 4b, we see that the total aerosol, including the troposphere, is also on a higher background level as well as in the stratosphere in Figure 4a. The tropopause can not be the main factor causing these differences as it was with the variability between the Free ensemble members as in that case the total sulfur load in Figure 4b would not be increased for *NdgWT*. This means that the sinks for SO_2 and sulfate aerosol are different in the respective simulations, since most of the sulfur emissions to the atmosphere are prescribed. These sources include volcanic eruptive and degassing emissions as well as anthropogenic and biomass burning emissions, and are exactly the same in every simulation. Only dimethyl sulfide (DMS) emissions are calculated online from a marine DMS climatology (Lana et al., 2011) as a function of wind speed (Nightingale et al., 2000), However, due to different surface wind patterns, DMS emissions are higher in *Free* than in *NdgWT*. Therefore DMS emissions cannot explain the higher background sulfur load in *NdgWT*. The sulfur sinks on the other hand are not prescribed. SO_2 can be oxidized to H_2SO_4 either as in the gas or aqueous phase and subsequently forms aerosols. Sulfur and particularly sulfate aerosol are removed from the atmosphere via wet and dry deposition (Kremser et al., 2016). Figure 5 is a schematic of the sulfur balance. The runs for this figure are taken from Feinberg et al. (2019), where the same modeling set-up was used with slight changes in the boundary conditions, which are now adjusted to the recommendations from ISA-MIP. We look at this period, since it is volcanically quiescent and representative for the background conditions. In Figure 5, the tropospheric oxidation flux of SO_2 in the aqueous phase (where SO_2 is directly linked to aerosol) is higher in the free running mode, whereas the flux over the gaseous pathway (oxidation to SO_3 and then H_2SO_4 with subsequent nucleation and condensation) is higher for the nudged mode. This suggests a larger abundance of liquid water in *Free*, or in other words more clouds. Aqueous converted sulfate aerosol is more likely to be removed from the atmosphere through wet deposition since it is already in-cloud. Thus, this explains why the tropospheric aerosol lifetime is shorter and the aerosol burden is smaller in free-running simulations (Table 3).

While nudging reduces internal variability it can in turn cause certain biases as well, which is caused by an inconsistency of the model dynamics and prescribed parameters. In other words, nudging introduces biases in temperatures, which causes changes in cloud formation (Zhang et al., 2014). This affects the hydrological cycle, namely convective and large scale precipitation. In nudged simulations, the convective precipitation was increased as opposed to a decrease in large scale precipitation (Lin et al., 2016). This is also the case with SOCOL-AERv2, as shown in Table 3. While convective precipitation enhances scavenging and wet deposition of aerosols, it is also an indicator for convective activity in general. In the tropical region, convection can lead to cross tropopause trans-

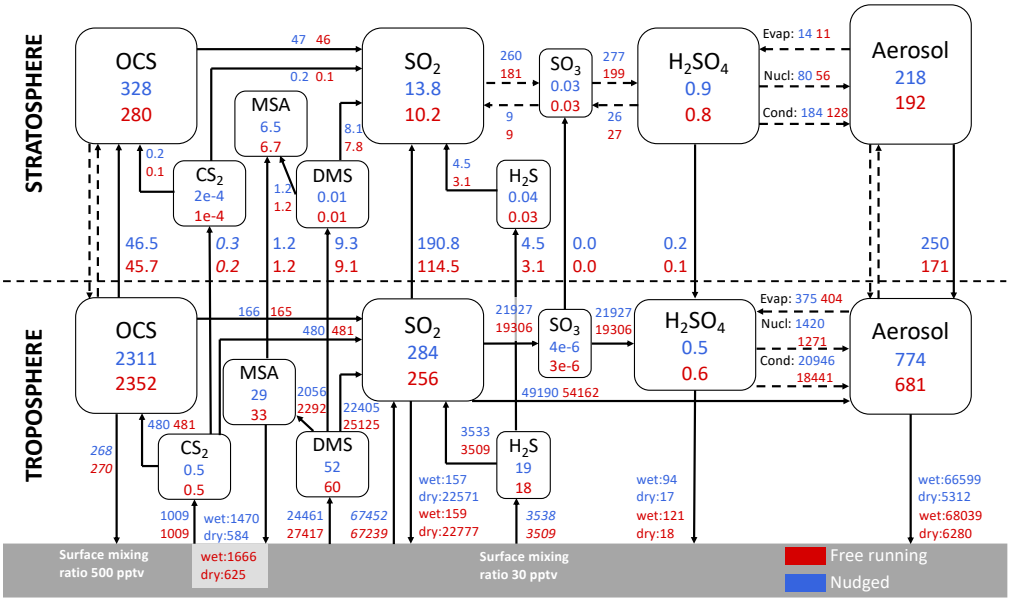

Figure 5. The sulfur fluxes as calculated by SOCOL-AERv2 for nudged and free running simulations for 2000–2010. from Feinberg et al. (2019), which used the same set-up as *Free1-3* and *NdgWT* except for some adjustment in boundary conditions to follow ISA-MIP recommendations. The units are in Gg S yr^{-1} for the fluxes and Gg S for the burdens.

Table 3. The large scale and convective precipitation as well as aerosol and OCS burdens for the free running model vs *NdgW* and *NdgWT*. All values are means over the whole time period from 2008 to 2012.

Simulation	**Large Scale Precipitation** (10^{-5} kg/m^{2}s)	**Convective Precipitation** (10^{-5} kg/m^{2}s)	**Tropospheric Aerosol (H_2SO_4)** (10^8 kg S)	**Stratospheric Aerosol (H_2SO_4)** (10^8 kg S)	**Stratospheric OCS** (10^8 kg S)
Free1	1.22 ± 0.04	2.08 ± 0.08	6.73 ± 0.97	2.29 ± 0.53	2.86 ± 0.15
Free2	1.22 ± 0.03	2.08 ± 0.07	6.80 ± 1.08	2.35 ± 0.54	2.84 ± 0.15
Free3	1.22 ± 0.03	2.08 ± 0.07	6.77 ± 0.99	2.19 ± 0.40	2.86 ± 0.15
NdgW	1.10 ± 0.06	2.13 ± 0.07	6.77 ± 0.90	2.38 ± 0.52	3.14 ± 0.19
NdgWT	1.05 ± 0.04	2.20 ± 0.08	7.59 ± 1.14	2.51 ± 0.52	3.33 ± 0.18

port, which is potentially the cause for a higher cross-tropopause transport of OCS and SO_2 and therefore a higher concentration of precursor gases for aerosol formation as seen in Figure 5 (Chin et al., 2000; Kremser et al., 2016). This could also be the reason for the higher peak for Nabro in Figure 4, since this was a tropical eruption and increased convection could have affected the cross-tropopause transport of the part of SO_2 that was emitted in the troposphere. It has to be noted that, although the analyzed changes in the global cloud parameters and sulfur burdens are consistent with each other, the temperature changes due to nudging also affect many other processes and parameters in the model besides clouds, such as microphysics, chemistry and transport in the stratosphere, which could've also contributed to the resulting differences, including the regional ones.

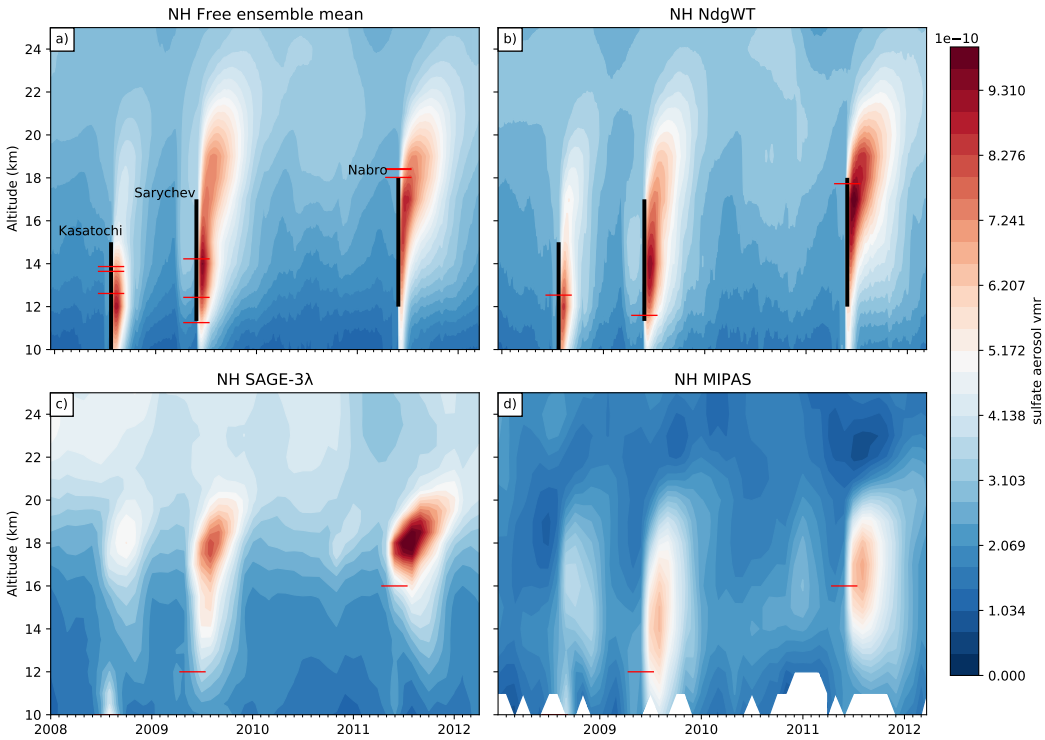

Figure 6. Northern hemispheric mean for the vertical distribution of sulfate aerosol volume mixing ratio (vmr) over time for *Free*, *NdgWT* as well as SAGE-3λ and MIPAS. The black vertical lines indicate the volcanic SO_2 plume as it is prescribed in the model, where the top was taken from VolcDB3 and are positioned at the time of the three main volcanic eruptions. The red horizontal lines indicate the tropopause height as calculated by SOCOL-AERv2 in (a) and (b) and from ERA-Interim in (c) and (d).

3.3.2 Spacial Distribution

Figure 6 shows the evolution of sulfate aerosol over time in the northern hemisphere over different altitudes. In SOCOL-AERv2, initial volcanic SO_2 plumes follow our set-up for the vertical distribution of volcanic emissions, which is the even distribution over the highest third above the volcano and the volcanic plume top, as the lowest point of the plume is not given in VolcDB3. As can be seen in Figure 6, this approach is rather coarse compared to observations, and in both SAGE-3λ and MIPAS, the sulfate aerosol is mostly dispersed over a smaller vertical range. Figure A1 suggests the altitudinal range is not so bad compared to MIPAS SO_2 profiles, but the resulting bias rather comes from the distribution within the vertical range, which looks more Gaussian in MIPAS. There is also a notably lower background for MIPAS at higher altitudes, especially when compared to SAGE-3λ, which may be part of the reason for the lower aerosol background conditions in Figure 4. Similar to Figure 4, the peaks here are again quite different but despite these differences, the lifetime for elevated aerosol burdens after the three eruptions is very similar for the simulations and observations.

In Figure 7, we present the sulfate aerosol evolution over time in the northern hemisphere. The northwards transport of all three events is depicted accurately by the model compared to both observations as well as an initial northwards and later southwards transport after the 2011 Nabro event. While background conditions look rather similar for *Free*, *NdgWT* and SAGE-3λ, the MIPAS background is visibly lower, which has already

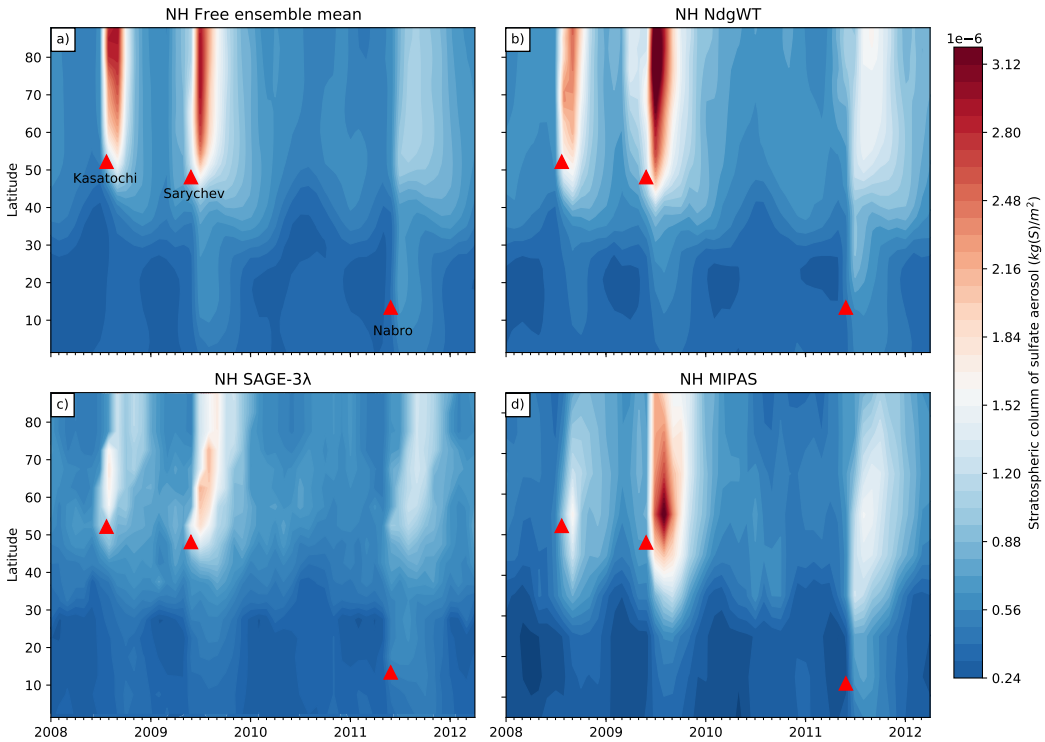

Figure 7. Northern hemispheric zonal mean aerosol evolution, integrated vertically above the tropopause for *Free*, *NdgWT*, SAGE-3λ and MIPAS. The triangles indicate the time and latitude at which the three main eruptions happened.

been observed in Figure 4. This is especially prevalent at lower latitudes. The MIPAS instrument had trouble picking up noise-free tropospheric signals and as the tropopause in the tropics can be significantly higher than 10 kilometres, missing data in the MIPAS dataset may be partly responsible for this low background bias in Figure 7 (Günther et al., 2018). Overall, from Figures 6 and 7 we can learn that *Free* and *NdgWT* are much closer to each other than to observations, and their difference is much smaller than the difference between the observations.

3.4 Increased Vertical Resolution

The atmospheric lifetime of volcanic aerosol is affected by several factors such as tropospheric wet removal, stratospheric transport and mixing or gravitational settling. As Sukhodolov et al. (2018) suggested that aerosol lifetime could be improved by an increased vertical resolution, Figure 8 compares the evolution of the total atmospheric sulfate aerosol for two nudged simulations with 39 and 90 vertical levels, *NdgW* and *NdgW90*. While the vertical resolution for both model set-ups is very similar in the boundary layer and in the mesosphere, it is about doubled around the extratropical tropopause and about tripled around the tropical tropopause as well as in the lower stratosphere in the 90 level version. This has a potential impact on the stratospheric fraction of the SO_2 emission profile, in particular for Nabro. The peak burdens for all three eruptions are very similar for the two simulations. Only for the Nabro eruption NdgW shows a slightly higher peak. A major difference however is the evolution after these main peaks. In *NdgW90*, the atmospheric aerosol lifetime for all three eruptions is longer than in NdgW. In particular after the Sarychev and Nabro eruption, *NdgW* is marked by a quick initial re-

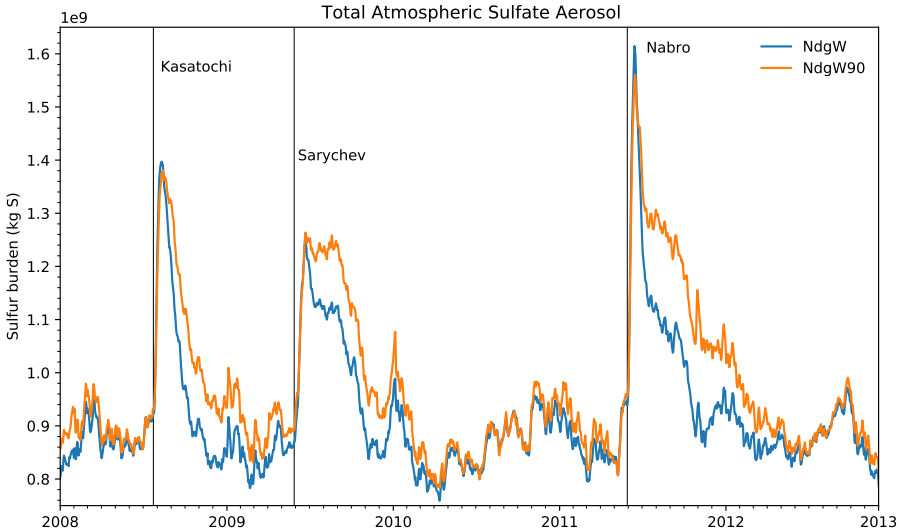

Figure 8. The evolution of atmospheric sulfate aerosol as daily means for the two simulations on 90 and 39 vertical levels respectively. Both simulations were nudged to observed horizontal wind fields.

moval. This indicates that the initial tropospheric wet removal is more pronounced in NdgW than in *NdgW90*.

To further elucidate differences in stratospheric transport and mixing processes on the aerosol lifetime after the Nabro eruption, two idealized simulations, *NdgIdeal39* and *NdgIdeal90*, have been analyzed. The SO_2 was emitted in a single gridbox in the tropics and in a single level at about 21km, the same day Nabro erupted in June 2011. The zonal mean aerosol distribution for both simulations after 100, 200 and 300 days is presented in Figure 9. After 100 days, the aerosol plume in *NdgIdeal39* is already clearly spread in the vertical and smoothed out, while in *NdgIdeal90* it is more constrained to a smaller vertical range with sharp gradients at the edge. This possibly contributes to the faster initial removal of aerosol after volcanic eruptions for *NdgW* compared to *NdgW90*, seen in Figure 8. Furthermore, *NdgIdeal39* shows 'leaking' to higher latitudes. From the water vapor tape recorder signal (Fig. A2), which is a measure of the net upward transport in the tropics (large-scale ascent and vertical diffusion, Mote et al., 1996), it becomes clear that the model version with 39 levels (*NdgWT39*) shows a faster transport than *NdgWT90*. As the residual vertical velocities (ω^*) in the tropical lower stratosphere are very similar (not shown), we conclude that the differences between both vertical resolutions are related to numerical diffusion processes. Even though most aerosol is transported to the northern hemisphere, there is also a slightly enhanced transport to the southern hemisphere in NdgIdeal39. After 200 days the tropical aerosol burden is clearly reduced in *NdgIdeal39*.

The vertical resolution effect was also described in Niemeier and Schmidt (2017) with the global chemistry climate model ECHAM5-HAM. There it is also argued that model versions with different vertical resolutions show mostly the same BDC strength, but at the same time the higher resolution model version has longer age of air in mid-latitudes and less vertically extent aerosol layer, which suggests an effect of the numerical diffusion that modulates the drainage of the tropical reservoir and the effectiveness of the aerosol transport by the shallow branch of the BDC. This could also partly ex-

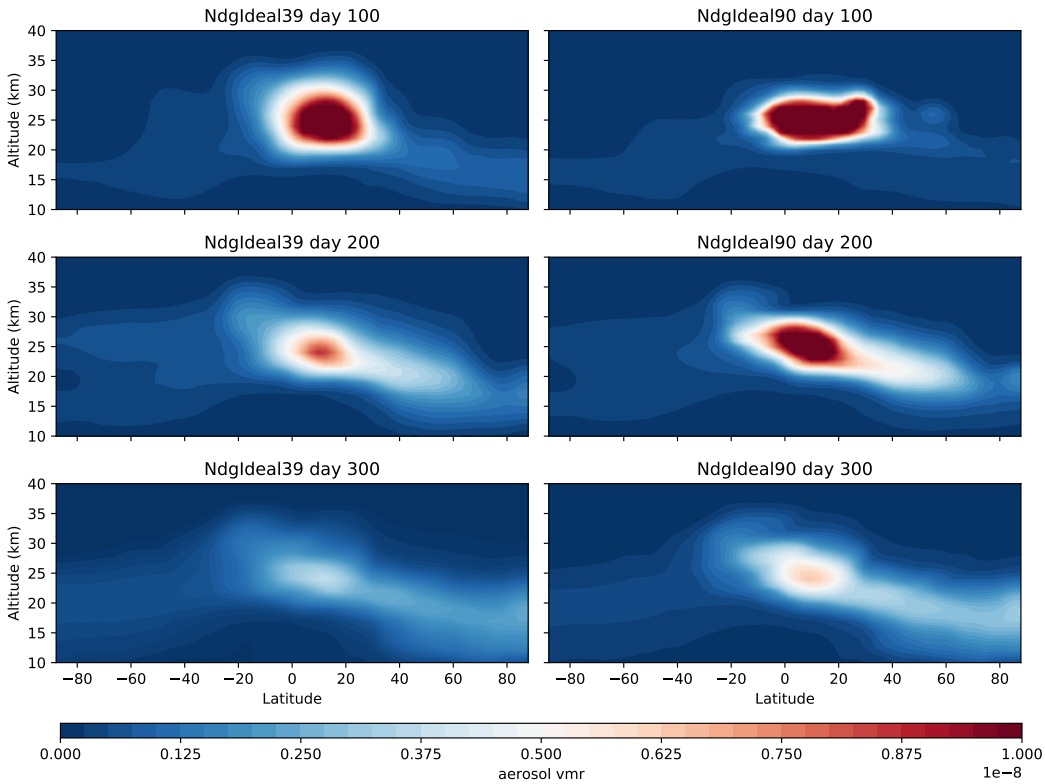

Figure 9. An idealized case of a volcanic eruption of the size of Nabro as it is transported meridionally in two simulations on 39 levels to the left and 90 levels to the right respectively. The SO_2 was emitted in a single grid cell and in a single level at ~21 km The values are zonal mean volume mixing ratios of H_2SO_4 up to an altitude of 40 km.

plain the missing 'plateau' in aerosol after the Pinatubo eruption which was shown to happen in modeling studies, including SOCOL-AERv2 in Sukhodolov et al. (2018) and Dhomse et al. (2020). On the other hand, in the present study with smaller volcanic events, the aerosol lifetime is already in good agreement with observations or even exceeded the latter, as seen in Figure 4 in Section 3.3. Important to note, also, that next to the effect on diffusion, the increased vertical resolution introduces other effects such as temperature changes (especially in the upper troposphere / lower stratosphere, Stevens et al., 2013) and thus affects many other processes controlling the lifetime of volcanic aerosol, like aerosol microphysics, chemistry, tropopause shape, etc..

4 Conclusions

The aim of this study was to analyze the capabilities of the model SOCOL-AERv2 to reproduce the observed stratospheric aerosol evolution after volcanic eruptions and to investigate the impact of uncertainties in emission datasets, observations, and the modeling set-up. Four databases for eruptive volcanic SO_2 emissions were compared initially to estimate the uncertainties in both the amount of initial SO_2 injection as well as the altitude of the volcanic plume. We showed that the different assumptions applied for the development of the databases lead to large differences in the modeled sulfur loading. Depending on the volcanic event, the peak sulfur burden varied by a factor of 1.3 to 2 between the different model simulations. This underlines the large model sensitivity to uncertainties in volcanic emission data, which are addressed within the ISA-MIP frame-

work. Further the internal model variability was investigated using a three members ensemble. The maximum increase in the stratospheric sulfur loading was found to differ between the ensemble members by up to a factor of two due to different tropopause heights, in particular in extratropical latitudes. A potential solution to this problem could be to prescribe the volcanic plume relative to the tropopause instead of using absolute values for the plume height.

In a third test, SOCOL-AERv2 was run with nudging the model dynamics to observed wind and temperature fields. In a nudged regime, we found an enhanced background sulfur burden. This is due to several factors. First, differences in the hydrological cycle, mainly cloud formation and precipitation, favor aqueous phase oxidation of SO_2 in free running simulations, which promotes wet aerosol scavenging, while gas phase oxidation dominates in nudged simulations. Second, convective activity appears to be stronger in nudged simulations which leads to an increased troposphere-to-stratosphere flux of sulfur-containing species. As model simulations in specified dynamics mode are proposed for the nowcasting of volcanic aerosol clouds, these differences in the atmospheric sulfur budget for background conditions would need to be considered.

Finally we investigated the influence of the model's vertical resolution on the aerosol evolution after the three volcanic eruptions. We show that initial tropospheric removal is likely decreased in the higher resolution simulations, since there is less vertical diffusion. Additionally, the aerosol is contained for a longer time within the tropical stratosphere, which increases its atmospheric residence time. This effect could potentially reproduce the plateau in aerosol loading observed after the Pinatubo eruption, which was not captured by the low vertical resolution model version in Sukhodolov et al. (2018) For the smaller events discussed here however, this may be undesirable in the current model set-up, since simulated aerosol lifetimes are already sufficiently close to or even longer than in the observations.

The conclusions drawn from the presented model evaluation hold for medium-sized volcanic eruptions, but could differ for more powerful eruptions as aerosol microphysics may be sensitive to the amount of the emitted material. For example, increased coagulation due to high initial particle number densities decreases aerosol lifetimes due to larger particle sizes and consequently faster sedimentation. Studying medium-sized events provides useful insights, but does not cover the full spectrum of potential interactions and feedbacks. For a comprehensive model evaluation, large eruptions have to be studied as well. This has been extensively done for Pinatubo, but observational uncertainties complicate coherent conclusions. Observational techniques have very much advanced within the past thirty years since the last major eruption, but there are still substantial uncertainties. In order to respond adequately to a large volcanic eruption and provide reliable model forecasts, observations would be required to be immediately available after the eruption. With Volcano Response (VolRES), there is already an initiative in place which aims at preparing for large volcanic eruptions. Furthermore, ISA-MIP seeks to bring modelers together within the same validation framework and to address the uncertainties in aerosol models in a more rigorous and comprehensive manner.

Appendix A

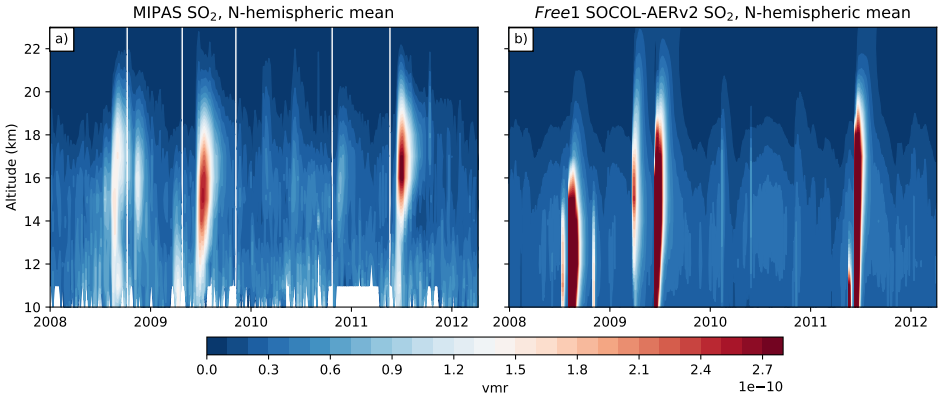

Figure A1. The northern hemispheric mean of SO_2 for (a) MIPAS in and (b) SOCOL-AERv2 (taken from the *Free1* simulation) as volume mixing ratio (vmr).

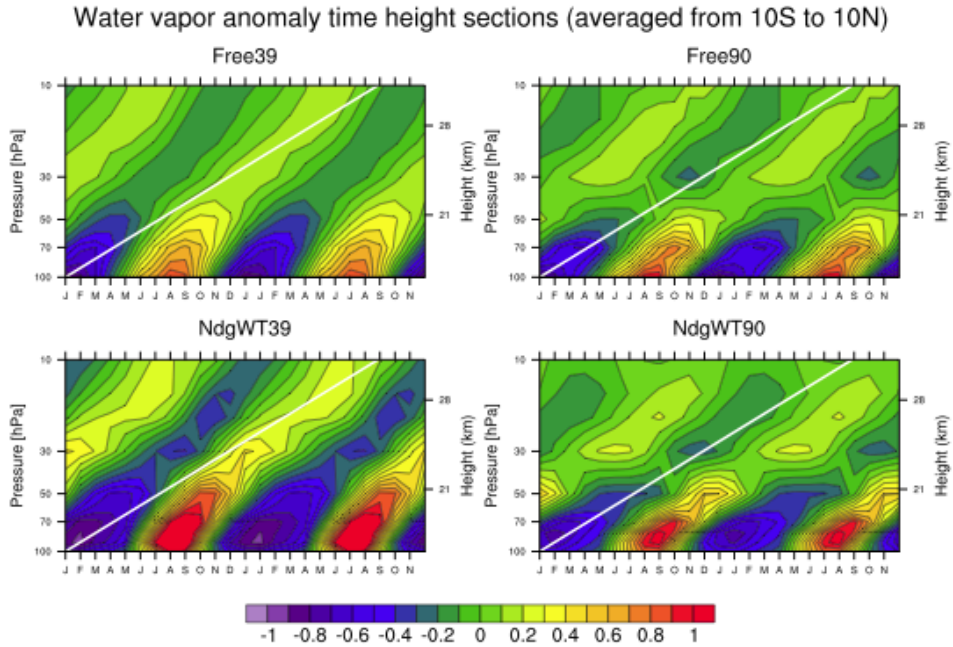

Figure A2. Time-height sections of water vapor mixing ratios averaged over 10 years shown as deviations from the mean profile, averaged between 10°N and 10°S for two free running simulations (upper panels) and two nudged simulations (lower panels), with 39 and 90 vertical levels, respectively. Two identical annual cycles are shown. The white line indicates the phase speed of the tape recorder signal derived from HALOE water vapor observations (Grooß & Russell III, 2005) for comparison.

Acknowledgments

This work was supported by the Swiss National Science Foundation (SNSF) under grants 200021_169241 (VEC) and 200020_182239 (POLE). All calculations with the SOCOL-AERv2 model were performed on the ETH Zürich cluster EULER. The SOCOL-AERv2 code and the simulation data are available from the first author or at `https://doi.org/10.5281/zenodo.5035442`. The MIPAS data sets for aerosol volume densities and SO_2 mixing ratios are available upon request from Michael Höpfner or at `http://www.imk-asf.kit.edu/english/308.php`. The CMIP6 sulfate aerosol data are available at `ftp://iacftp.ethz.ch/pub_read/luo/CMIP6/`. Volcanic forcing data from different databases are accessible through the ISA-MIP website: `http://isamip.eu/input`. ER and TS also represent the SPbSU "Ozone Layer and Upper Atmosphere Research" laboratory supported by the Ministry of Science and Higher Education of the Russian Federation under agreement 075-15-2021-583. AF was supported by the ETH grant ETH-39 15-2.

References

Andersson, S. M., Martinsson, B. G., Vernier, J.-P., Friberg, J., Brenninkmeijer, C. A., Hermann, M., ... Zahn, A. (2015). Significant radiative impact of volcanic aerosol in the lowermost stratosphere. *Nature Communications*, *6*. doi: 10.1038/ncomms8692

Andres, R., & Kasgnoc, A. (1998). A time-averaged inventory of subaerial volcanic sulfur emissions. *Journal of Geophysical Research: Atmospheres*, *103*(D19), 25251–25261. doi: 10.1029/98JD02091

Arfeuille, F., Luo, B. P., Heckendorn, P., Weisenstein, D., Sheng, J. X., Rozanov, E., ... Peter, T. (2013). Modeling the stratospheric warming following the mt. pinatubo eruption: uncertainties in aerosol extinctions. *Atmospheric Chemistry and Physics*, *13*(22), 11221–11234. doi: 10.5194/acp-13-11221-2013

Bingen, C., Robert, C. E., Stebel, K., Brühl, C., Schallock, J., Vanhellemont, F., ... Pinnock, S. (2017). Stratospheric aerosol data records for the climate change initiative: Development, validation and application to chemistry-climate modelling. *Remote Sensing of Environment*, *203*, 296–321. doi: 10.1016/j.rse.2017.06.002

Brühl, C. (2018). Volcanic SO_2 data derived from limb viewing satellites for the lower stratosphere from 1998 to 2012, and from nadir viewing satellites for the troposphere. *World Data Center for Climate (WDCC) at DKRZ*. doi: 10.1594/WDCC/SSIRC_1

Brühl, C., Lelieveld, J., Tost, H., Höpfner, M., & Glatthor, N. (2015). Stratospheric sulfur and its implications for radiative forcing simulated by the chemistry climate model EMAC. *Journal of Geophysical Research: Atmospheres*, *120*(5), 2103–2118. doi: 10.1002/2014JD022430

Butchart, N. (2014). The Brewer-Dobson circulation. *Reviews of Geophysics*, *52*(2), 157–184. doi: 10.1002/2013RG000448

Carn, S. (2019). Multi-Satellite Volcanic Sulfur Dioxide L4 Long-Term Global Database V3. *Greenbelt, MD, USA, Goddard Earth Science Data and Information Services Center (GES DISC)*. doi: 10.5067/MEASURES/SO2/DATA404

Carn, S. A., Clarisse, L., & Prata, A. J. (2016). Multi-decadal satellite measurements of global volcanic degassing. *Journal of Volcanology and Geothermal Research*, *311*, 99–134. doi: 10.1016/j.jvolgeores.2016.01.002

Chin, M., Rood, R. B., Lin, S.-J., Müller, J.-F., & Thompson, A. M. (2000). Atmospheric sulfur cycle simulated in the global model GOCART: Model description and global properties. *Journal of Geophysical Research: Atmospheres*, *105*(D20), 24671–24687. doi: 10.1029/2000JD900384

Chrysanthou, A., Maycock, A. C., Chipperfield, M. P., Dhomse, S., Garny, H., Kinnison, D., ... Yamashita, Y. (2019). The effect of atmospheric nudging on the stratospheric residual circulation in chemistry-climate models. *Atmospheric*

Chemistry and Physics, *19*, 11559–11586. doi: 10.5194/acp-19-11559-2019

Clarisse, L., Coheur, P.-F., Theys, N., Hurtmans, D., & Clerbaux, C. (2014). The 2011 Nabro eruption, a SO_2 plume height analysis using IASI measurements. *Atmospheric Chemistry and Physics*, *14*, 3095–3111. doi: 10.5194/acp-14-3095-2014

Crutzen, P. J. (2006). Albedo Enhancement by Stratospheric Sulfur Injections: A Contribution to Resolve a Policy Dilemma? *Climatic Change*, *77*(211). doi: 10.1007/s10584-006-9101-y

de Leeuw, J., Schmidt, A., Witham, C. S., Theys, N., Taylor, I. A., Grainger, R. G., … Kristiansen, N. I. (2020). The 2019 Raikoke volcanic eruption: Part 1 Dispersion model simulations and satellite retrievals of volcanic sulfur dioxide. *Atmospheric Chemistry and Physics Discussions*. doi: 10.5194/acp-2020-889

Dee, D. P., Uppala, S. M., Simmons, A. J., Berrisford, P., Poli, P., Kobayashi, U., S. Andrae, … F, V. (2011). The ERA-Interim reanalysis: Configuration and performance of the data assimilation system. *Quarterly Journal of the Royal Meteorological Society*, *137*(656), 553–597. doi: 10.1002/qj.828

Dentener, F., Kinne, S., Bond, T., Boucher, O., Cofala, J., Generoso, S., … Wilson, J. (2006). Emissions of primary aerosol and precursor gases in the years 2000 and 1750 prescribed data-sets for AeroCom. *Atmospheric Chemistry and Physics*, *6*(12), 4321–4344. doi: 10.5194/acp-6-4321-2006

Dhomse, S. S., Mann, G. W., Antuña Marrero, J. C., Shallcross, S. E., Chipperfield, M. P., Carslaw, K. S., … Johnson, C. E. (2020). Evaluating the simulated radiative forcings, aerosol properties, and stratospheric warmings from the 1963 Mt Agung, 1982 El Chichón, and 1991 Mt Pinatubo volcanic aerosol clouds. *Atmospheric Chemistry and Physics*, *20*(21), 13627–13654. doi: 10.5194/acp-20-13627-2020

Diallo, M., Ploeger, F., Konopka, P., Birner, T., Müller, R., Riese, M., … Jegou, F. (2017). Significant Contributions of Volcanic Aerosols to Decadal Changes in the Stratospheric Circulation. *Geophysical Research Letters*, *44*(20), 10780–10791. doi: 10.1002/2017GL074662

Diehl, T., Heil, A., Chin, M., Pan, X., Streets, D., Schultz, M., & Kinne, S. (2012). Anthropogenic, biomass burning, and volcanic emissions of black carbon, organic carbon, and SO_2 from 1980 to 2010 for hindcast model experiments. *Atmospheric Chemistry and Physics Discussions*, *12*, 24895–24954. doi: 10.5194/acpd-12-24895-2012

Dutton, E. G., & Christy, J. R. (1992). Solar Radiative Forcing At Selected Locations and Evidence for global lower tropospheric cooling following the eruptions of El Chichón and Pinatubo. *Geophysical Research Letters*, *19*(23), 2313–2316. doi: 10.1029/92GL02495

Eyring, V., Bony, S., Meehl, G. A., Senior, C. A., Stevens, B., Stouffer, R. J., & Taylor, K. E. (2016). Overview of the Coupled Model Intercomparison Project Phase 6 (CMIP6) experimental design and organization. *Geoscientific Model Development*, *9*(5), 1937–1958. doi: 10.5194/gmd-9-1937-2016

Feinberg, A., Sukhodolov, T., Luo, B.-P., Rozanov, E., Winkel, L. H., Peter, T., & Stenke, A. (2019). Improved tropospheric and stratospheric sulfur cycle in the aerosol-chemistry-climate model SOCOL-AERv2. *Geoscientific Model Development*, *12*(9), 3863–3887. doi: 10.5194/gmd-12-3863-2019

Fromm, M., Nedoluha, G., & Charvát, Z. (2013). Comment on "Large Volcanic Aerosol Load in the Stratosphere Linked to Asian Monsoon Transport". *Science*, *339*(6120), 647. doi: 10.1126/science.1228605

Gettelman, A., Hegglin, M. I., Son, S.-W., Kim, J., Fujiwara, M., Birner, T., … Tian, W. (2010). Multimodel assessment of the upper troposphere and lower stratosphere: Tropics and global trends. *Journal of Geophysical Research: Atmospheres*, *115*(D3). doi: 10.1029/2009JD013638

Graf, H., Langmann, B., & Feichter, J. (1998). The contribution of Earth degassing

to the atmospheric sulfur budget. *Chemical Geology*, *147*, 131–145. doi: 10.1016/S0009-2541(97)00177-0

Granier, C., Bessagnet, B., Bond, T., D'Angiola, A., van der Gon, H. D., Frost, G. J., ... van Vuuren, D. P. (2011). Evolution of anthropogenic and biomass burning emissions of air pollutants at global and regional scales during the 1980-2010 period. *Climatic Change*, *109*(163), 163–190. doi: 10.1007/s10584-011-0154-1

Grooß, J.-U., & Russell III, J. M. (2005). Technical note: A stratospheric climatology for O_3, H_2O, CH_4, NO_x, HCl and HF derived from HALOE measurements. *Atmospheric Chemistry and Physics*, *5*(10), 2797–2807. doi: 10.5194/acp-5-2797-2005

Günther, A., Höpfner, M., Sinnhuber, B.-M., Griessbach, S., Deshler, T., von Clarmann, T., & Stiller, G. (2018). MIPAS observations of volcanic sulfate aerosol and sulfur dioxide in the stratosphere. *Atmospheric Chemistry and Physics*, *18*(2), 1217–1239. doi: 10.5194/acp-18-1217-2018

Höpfner, M., Boone, C. D., Funke, B., Glatthor, N., Grabowski, U., Günther, A., ... Wissmüller, K. (2015). Sulfur dioxide (SO_2) from MIPAS in the upper troposphere and lower stratosphere 2002-2012. *Atmospheric Chemistry and Physics*, *15*(12), 7017–7037. doi: 10.5194/acp-15-7017-2015

Jeuken, A. B. M., Siegmund, P. C., Heijboer, L. C., Feichter, J., & Bengtsson, L. (1996). On the potential of assimilating meteorological analyses in a global climate model for the purpose of model validation. *Journal of Geophysical Research: Atmospheres*, *101*(D12), 16939–16950. doi: 10.1029/96JD01218

Kettle, A. J., & Andreae, M. O. (2000). Flux of dimethylsulfide from the oceans: A comparison of updated data sets and flux models. *Journal of Geophysical Research: Atmospheres*, *105*(D22), 26793–26808. doi: 10.1029/2000JD900252

Kettle, A. J., Andreae, M. O., Amouroux, D., Andreae, T. W., Bates, T. S., Berresheim, H., ... Uher, G. (1999). A global database of sea surface dimethylsulfide (DMS) measurements and a procedure to predict sea surface DMS as a function of latitude, longitude, and month. *Global Biogeochemical Cycles*, *13*(2), 399–444. doi: 10.1029/1999GB900004

Konopka, P., Ploeger, F., Tao, M., Birner, T., & M., R. (2015). Hemispheric asymmetries and seasonality of mean age of air in the lower stratosphere: Deep versus shallow branch of the Brewer-Dobson circulation. *Journal of Geophysical Research: Atmospheres*, *120*(5), 2053–2066. doi: 10.1002/2014JD022429

Kremser, S., Thomason, L. W., von Hobe, M., Hermann, M., Deshler, T., Timmreck, C., ... Meland, B. (2016). Stratospheric aerosol-Observations, processes, and impact on climate. *Reviews of Geophysics*, *54*(2), 278–335. doi: 10.1002/2015RG000511

Lana, A., Bell, T. G., Simó, R., Vallina, S. M., Ballabrera-Poy, J., Kettle, A. J., ... Liss, P. S. (2011). An updated climatology of surface dimethlysulfide concentrations and emission fluxes in the global ocean. *Global Biogeochemical Cycles*, *25*(1), GB1004. doi: 10.1029/2010GB003850

Lin, G., Wan, H., Zhang, K., Qian, Y., & Ghan, S. J. (2016). Can nudging be used to quantify model sensitivities in precipitation and cloud forcing? *Jurnal of Advances in Modeling Earth Systems*, *8*(3), 1073–1091. doi: 10.1002/2016MS000659

MacMartin, D. G., Ricke, K. L., & Keith, D. W. (2018). Solar geoengineering as part of an overall strategy for meeting the 1.5°C Paris target. *Philosophical Transactions of the Royal Society A: Mathematical, Physical and Engineering Sciences*, *376*. doi: 10.1098/rsta.2016.0454

McCormick, M., Thomason, L., & Trepte, C. (1995). Atmospheric effects of the Mt Pinatubo eruption. *Nature*, *373*, 399–404. doi: 10.1038/373399a0

Mills, M. J., Schmidt, A., Easter, R., Solomon, S., Kinnison, D. E., Ghan, S. J., ... Gettelman, A. (2016). Global volcanic aerosol properties derived from emis-

sions, 1990-2014, using CESM1(WACCM). *Journal of Geophysical Research: Atmospheres*, *121*(5), 2332–2348. doi: 10.1002/2015JD024290

Montzka, S. A., Calvert, P., Hall, B. D., Elkins, J. W., Conway, T. J., Tans, P. P., & Sweeney, C. (2007). On the global distribution, seasonality, and budget of atmospheric carbonyl sulfide (cos) and some similarities to co_2. *Journal of Geophysical Research: Atmospheres*, *112*(D9). doi: 10.1029/2006JD007665

Mote, P., Rosenlof, K., Mclntyre, M., Carr, E., Gille, J., Holton, J., ... Waters, J. (1996). An atmospheric tape recorder: The imprint of tropical tropopause temperatures on stratospheric water vapor. *Journal of Geophysical Research: Atmoshperes*, *101*(D2), 3989–4006. doi: 10.1029/95JD03422

Muthers, S., Anet, J. G., Stenke, A., Raible, C. C., Rozanov, E., Brönnimann, S., ... Schmutz, W. (2014). The coupled atmosphere-chemistry-ocean model SOCOL-MPIOM. *Geoscientific Model Developement*, *7*(5), 2157–2179. doi: 10.5194/gmd-7-2157-2014

Neely, R. R., & Schmidt, A. (2016). Volcaneesm (volcanic emissions for earth system models): Volcanic sulphur dioxide (so_2) emissions database from 1850 to present. *Centre for Environmental Data Analysis*. Retrieved from `http://catalogue.ceda.ac.uk/uuid/bfbd5ec825fa422f9a858b14ae7b2a0d`

Niemeier, U., & Schmidt, H. (2017). Changing transport processes in the stratosphere by radiative heating of sulfate aerosols. *Atmospheric Chemistry and Physics*, *17*(24), 14871–14886. doi: 10.5194/acp-17-14871-2017

Nightingale, P. D., Malin, G., Law, C. S., Watson, A. J., Liss, P. S., Liddicoat, M. I., ... Upstill-Goddard, R. C. (2000). In situ evaluation of air-sea gas exchange parameterizations using novel conservative and volatile tracers. *Global Biogeochemical Cycles*, *14*(1), 373–387. doi: 10.1029/1999GB900091

Proctor, J., Hsiang, S., Burney, J., Burke, M., & Schlenker, W. (2018). Estimating global agricultural effects of geoengineering using volcanic eruptions. *Nature*, *560*, 480–483. doi: 10.1038/s41586-018-0417-3

Raible, C. C., Brönnimann, S., Auchmann, R., Brohan, P., Frölicher, T. L., Graf, H.-F., ... Wegmann, M. (2016). Tambora 1815 as a test case for high impact volcanic eruptions: Earth system effects. *WIREs Climate Change*, *7*(4), 569–589. doi: 10.1002/wcc.407

Rayner, N. A., Parker, D. E., Horton, E. B., Folland, C. K., Alexander, L. V., Rowell, D. P., ... Kaplan, A. (2003). Global analyses of sea surface temperature, sea ice, and night marine air temperature since the late nineteenth century. *Journal of Geophysical Research: Atmospheres*, *108*(D14). doi: 10.1029/2002jd002670

Revell, L. E., Stenke, A., Luo, B., Kremser, S., Rozanov, E., Sukhodolov, T., & Peter, T. (2017). Impacts of Mt Pinatubo volcanic aerosol on the tropical stratosphere in chemistry-climate model simulations using CCMI and CMIP6 stratospheric aerosol data. *Atmospheric Chemistry and Physics*, *17*(21), 13139–13150. doi: 10.5194/acp-17-13139-2017

Ridley, D. A., Solomon, S., Barnes, J. E., Burlakov, V. D., Deshler, T., Dolgii, S. I., ... Vernier, J. (2014). Total volcanic stratospheric aerosol optical depths and implications for global climate change. *Geophysical Research Letters*, *41*(22), 7763–7769. doi: 10.1002/2014GL061541

Sheng, J.-X., Weisenstein, D. K., Luo, B.-P., Rozanov, E., Stenke, A., Anet, J., ... Peter, T. (2015). Global atmospheric sulfur budget under volcanically quiescent conditions: Aerosol-chemistry-climate model predictions and validation. *Journal of Geophysical Research: Atmospheres*, *120*(1), 256–276. doi: 10.1002/2014JD021985

Stenke, A., Schraner, M., Rozanov, E., Egorova, T., Luo, B., & Peter, T. (2013). The SOCOL version 3.0 chemistry-climate model: Description, evaluation, and implications from an advanced transport algorithm. *Geoscientific Model Development*, *6*(5), 1407–1427. doi: 10.5194/gmd-6-1407-2013

Stevens, B., Giorgetta, M., Esch, M., Mauritsen, T., Crueger, T., Rast, S., ... Roeckner, E. (2013). Atmospheric component of the MPI-M Earth System Model: ECHAM6. *Journal of Advances in Modeling Earth Systems*, *5*, 146–172. doi: 10.1002/jame.20015

Sukhodolov, T., Egorova, T., Stenke, A., Ball, W. T., Brodowsky, C., Chiodo, G., ... Rozanov, E. (2021). Atmosphere-Ocean-Aerosol-Chemistry-Climate Model SOCOLv4.0: description and evaluation. *Geoscientific Model Development Discussions*. doi: 10.5194/gmd-2021-35

Sukhodolov, T., Sheng, J. X., Feinberg, A., Luo, B. P., Peter, T., Revell, L., ... Rozanov, E. (2018). Stratospheric aerosol evolution after Pinatubo simulated with a coupled size-resolved aerosol-chemistry-climate model, SOCOL-AERv1.0. *Geoscientific Model Development*, *11*(7), 2633–2647. doi: 10.5194/gmd-11-2633-2018

Swingedouw, D., Mignot, J., Ortega, P., Khodri, M., Menegoz, M., Cassou, C., & Hanquiez, V. (2017). Impact of explosive volcanic eruptions on the main climate variability modes. *Global and Planetary Change*, *150*, 24–45. doi: 10.1016/j.gloplacha.2017.01.006

Theys, N., Campion, R., Clarisse, L., Brenot, H., van Gent, J., Dils, B., ... Ferrucci, F. (2013). Volcanic SO_2 fluxes derived from satellite data: A survey using OMI, GOME-2, IASI and MODIS. *Atmospheric Chemistry and Physics*, *13*(12), 5945–5968. doi: 10.5194/acp-13-5945-2013

Thomason, L. W., Ernest, N., Millán, L., Rieger, L., Bourassa, A., Vernier, J. P., ... Peter, T. (2018). A global space-based stratospheric aerosol climatology: 1979-2016. *Earth System Science Data*, *10*(1), 469–492. doi: 10.5194/essd-10-469-2018

Timmreck, C. (2012). Modeling the climatic effects of large explosive volcanic eruptions. *WIREs: Climate Change*, *3*(6), 545–564. doi: 10.1002/wcc.192

Timmreck, C., Mann, G. W., Aquila, V., Hommel, R., Lee, L. A., Schmidt, A., ... Weisenstein, D. (2018). The Interactive Stratospheric Aerosol Model Intercomparison Project (ISA-MIP): motivation and experimental design. *Geoscientific Model Development*, *11*(7), 2581–2608. doi: 10.5194/gmd-11-2581-2018

Toohey, M., Krüger, K., Niemeier, U., & Timmreck, C. (2011). The influence of eruption season on the global aerosol evolution and radiative impact of tropical volcanic eruptions. *Atmospheric Chemistry and Physics*, *11*(23), 12351–12367. doi: 10.5194/acp-11-12351-2011

Trenberth, K. E., & Dai, A. (2007). Effects of Mount Pinatubo volcanic eruption on the hydrological cycle as an analog of geoengineering. *Geophysical Research Letters*, *34*(15). doi: 10.1029/2007GL030524

Vernier, J.-P., Thomason, L., Fairlie, T. D., Minnis, P., Palikonda, R., & Bedka, K. M. (2013). Comment on "Large Volcanic Aerosol Load in the Stratosphere Linked to Asian Monsoon Transport". *Science*, *339*(6120), 647. doi: 10.1126/science.1227817

von Savigny, C., Timmreck, C., Buehler, S. A., Burrows, J. P., Giorgetta, M., Hegerl, G., ... Vogel, B. (2020). The Research Unit VolImpact: Revisiting the volcanic impact on atmosphere and climate - preparations for the next big volcanic eruption. *Meteorologische Zeitschrift (Contributions to Atmospheric Sciences)*, *29*(1), 3–18. doi: 10.1127/metz/2019/0999

Weisenstein, D. K., Yue, G. K., Ko, M. K. W., Sze, N.-D., Rodriguez, J. M., & Scott, C. J. (1997). A two-dimensional model of sulfur species and aerosols. *Journal of Geophysical Research*, *102*(D11), 13019–13035. doi: 10.1029/97JD00901

Zanchettin, D., Khodri, M., Timmreck, C., Toohey, M., Schmidt, A., Gerber, E. P., ... Tummon, F. (2016). The Model Intercomparison Project on the climatic response to Volcanic forcing (VolMIP): Experimental design and forcing input data for CMIP6. *Geoscientific Model Development*, *9*(8), 2701–2719. doi:

10.5194/gmd-9-2701-2016

Zhang, K., Wan, H., Liu, X., Ghan, S. J., Kooperman, G. J., Ma, P.-L., ... Lohmann, U. (2014). Technical Note: On the use of nudging for aerosol-climate model intercomparison studies. *Atmospheric Chemistry and Physics*, *14*(16), 8631–8645. doi: 10.5194/acp-14-8631-2014